

1 **Stochastic Parameterization: Towards a new view of**
2 **Weather and Climate Models**

3 JUDITH BERNER*

4 *National Center for Atmospheric Research[†], Boulder, Colorado*

5 ULRICH ACHATZ

6 *Institut für Atmosphäre und Umwelt, Goethe-Universität, Frankfurt am Main, Germany*

7 LAURIANE BATTÉ

8 *CNRM-GAME, Météo-France/CNRS, Toulouse, France*

9 LISA BENGTSSON

10 *Swedish Meteorological and Hydrological Institute, Norrköping, Sweden*

11 ALVARO DE LA CÁMARA

12 *National Center for Atmospheric Research Boulder, Colorado*

13 HANNAH M. CHRISTENSEN

14 *University of Oxford, Atmospheric, Oceanic and Planetary Physics, Oxford*

15 MATTEO COLANGELI

16 *Gran Sasso Science Institute, Viale F. Crispi 7, 67100 L'Aquila, Italy*

17 DANIELLE R. B. COLEMAN

18 *National Center for Atmospheric Research[†], Boulder, Colorado*

19 DAAN CROMMELIN

20 *CWI Amsterdam, the Netherlands and Korteweg-de Vries Institute for Mathematics,*
21 *University of Amsterdam*

* *Corresponding author address:* Judith Berner, NCAR, P.O.Box 3000, Boulder, CO 80303. E-mail: berner@ucar.edu

[†] NCAR is sponsored by the National Science Foundation

22
23
24
25
26
27
28
29
30
31
32
33
34
35
36
37
38
39
40
41
42
43
44
45
46
47

STAMEN I. DOLAPTCHIEV

Institut für Atmosphäre und Umwelt, Goethe-Universität, Frankfurt am Main, Germany

CHRISTIAN L.E. FRANZKE

*Meteorological Institute and Centre for Earth System Research and Sustainability (CEN),
University of Hamburg, Hamburg, Germany*

PETRA FRIEDERICHS

Meteorological Institute, University of Bonn, Germany

PETER IMKELLER

Institut für Mathematik, Humboldt-Universität zu Berlin, Berlin, Germany

HEIKKI JÄRVINEN

University of Helsinki, Department of Physics, Helsinki, Finland

STEPHAN JURICKE

University of Oxford, Atmospheric, Oceanic and Planetary Physics, Oxford

VASSILI KITSIOS

*CSIRO Oceans and Atmosphere Flagship, 107-121 Station St, Aspendale, Victoria 3195,
AUSTRALIA*

FRANÇOIS LOTT

*Laboratoire de Météorologie Dynamique (CNRS/IPSL), Ecole Normale Supérieure, Paris,
France*

VALERIO LUCARINI

*Meteorological Institute Centre for Earth System Research and Sustainability (CEN), University
of Hamburg, Hamburg, Germany; Department of Mathematics and Statistics, University of
Reading, Reading, UK*

SALIL MAHAJAN

Oak Ridge National Laboratory, USA

TIMOTHY N. PALMER

48 *University of Oxford, Atmospheric, Oceanic and Planetary Physics, Oxford*

49 CÉCILE PENLAND

50 *Physical Sciences Division, NOAA/Earth System Research Laboratory, Boulder, Colorado*

51 MIRJANA SAKRADZIJA

52 *Max Planck Institute for Meteorology and Hans-Ertel Centre for Weather Research, Deutscher*
53 *Wetterdienst, Hamburg, Germany*

54 JIN-SONG VON STORCH

55 *Max-Planck Institute for Meteorology, Hamburg*

56 ANTJE WEISHEIMER

57 *National Centre for Atmospheric Science (NCAS), University of Oxford, Atmospheric, Oceanic*
58 *and Planetary Physics, Oxford, and ECMWF, Shinfield Park, Reading, UK*

59 MICHAEL WENIGER

60 *Meteorological Institute, University of Bonn, Germany*

61 PAUL D. WILLIAMS

62 *Department of Meteorology, University of Reading, Reading, UK*

63 JUN-ICHI YANO

64 *GAME-CNRM, CNRS, Météo-France, 42 Av. Coriolis, Toulouse, France*

65

66 **ABSTRACT**

67 The last decade has seen the success of stochastic parameterizations in short-term, medium-
68 range and seasonal forecasts: operational weather centers now routinely use stochastic
69 parameterization schemes to better represent model inadequacy and improve the quantification
70 of forecast uncertainty. Developed initially for numerical weather prediction, the inclusion of
71 stochastic parameterizations not only provides better estimates of uncertainty, but it is also
72 extremely promising for reducing longstanding climate biases and relevant for determining the
73 climate response to external forcing.

74 This article highlights recent developments from different research groups which show that the
75 stochastic representation of unresolved processes in the atmosphere, oceans, land surface and
76 cryosphere of comprehensive weather and climate models (a) gives rise to more reliable
77 probabilistic forecasts of weather and climate and (b) reduces systematic model bias.

78 We make a case that the use of mathematically stringent methods for the derivation of stochastic
79 dynamic equations will lead to substantial improvements in our ability to accurately simulate
80 weather and climate at all scales. Recent work in mathematics, statistical mechanics and
81 turbulence is reviewed, its relevance for the climate problem demonstrated, and future research
82 directions outlined.

83

84 **CAPSULE** (20-30 words)

85 Stochastic parameterizations - empirically derived, or based on rigorous mathematical and

86 statistical concepts - have great potential to increase the predictive capability of next generation

87 weather and climate models.

88 **1 The need for stochastic parameterizations**

89 Numerical weather and climate modeling is based on the discretization of the continuous
90 equations of motion. Such models can be characterized in terms of their dynamical core, which
91 describes the resolved scales of motion, and the physical parameterizations, which provide
92 estimates of the grid-scale effect of processes, that cannot be resolved. This general approach
93 has been hugely successful in that skillful predictions of weather and climate are now routinely
94 made (e.g. Bauer et al. 2015). However, it has become apparent through the verification of these
95 predictions that current state-of-the-art models still exhibit persistent and systematic
96 shortcomings due to an inadequate representation of unresolved processes.

97 Despite the continuing increase of computing power, which allows numerical weather and
98 climate prediction models to be run with ever higher resolution, the multi-scale nature of
99 geophysical fluid dynamics implies that many important physical processes (e.g. tropical
100 convection, gravity wave drag, micro-physical processes) are still not resolved.
101 Parameterizations of sub-grid-scale processes contain closure assumptions, and related
102 parameters with inherent uncertainties. Although increasing model resolution gradually
103 pushes these assumptions further down the spectrum of motions, it is realistic to assume
104 that some form of closure or physical parameterization will be present in simulation models
105 into the foreseeable future.

106 Moreover, for climate simulations, a decision must be made as to whether computational
107 resources should be used to increase the representation of sub-grid physical processes or to build
108 a comprehensive Earth-System Model, by including additional climate components such as the
109 cryosphere, chemistry and biosphere. In addition, the decision must be made about whether
110 computational resources should go towards increased horizontal, vertical and temporal

111 resolution or additional ensemble members.

112 Additional challenges are posed by intrinsically coupled phenomena like the Madden-Julian
113 Oscillation (MJO) and tropical cyclones. Correctly simulating these tropical multi-scale
114 features requires resolving or accurately representing small-scale processes such as
115 convection in addition to capturing the large-scale response and feedback. Many of the
116 Coupled Model Intercomparison Project phase 5 (CMIP5) climate models still do not properly
117 simulate the MJO and convectively coupled waves (Hung et al. 2013).

118 A great challenge is posed by the representation of partially resolved processes (either in the
119 time or space domain). The range of scales on which a physical process is only partially
120 resolved is often referred to as the “gray zone” (e.g. Gerard 2007). In this gray zone, the number
121 of eddies in each grid box is no longer large enough to fulfill the “law of large numbers”
122 underlying deterministic bulk parameterizations and a stochastic approach becomes essential.

123 An example for a partially resolved process is convection, which is often split into a resolved
124 (large-scale) and parameterized component (e.g. Arakawa 2004). The equilibrium assumption
125 no longer holds when the model resolution is increased such that a clear scale separation
126 between convection and larger scales no longer is valid (e.g. Yano and Plant 2012a,b). In this
127 case the subgrid-scale parameterization takes a prognostic form rather than being diagnostic, as
128 explicitly shown for the mass-flux formulation by Yano (2014).

129 As the next generation of numerical models attempts to seamlessly predict weather as well as
130 climate, there is an increasing need to develop parameterizations that adapt automatically to
131 different spatial scales (“scale-aware parameterizations”). A big advantage of the
132 mathematically rigorous approach is that the subgrid-model is valid for increasing spatial
133 resolutions within a range of scales that is obtained as part of the derivation.

134 Mathematical approaches to stochastic modeling rely on the assumption that a physical
135 system can be expressed in terms of variables of interest, and variables which one does not
136 want to explicitly resolve. In the mathematical literature this is usually referred to as the
137 operation of coarse-graining and performed through the method of homogenization
138 (Papanicolaou and Kohler 1974, Gardiner 1985, Pavliotis and Stuart 2008). The goal is then
139 to derive an effective equation for the slow predictable processes and to represent the effect
140 of the now unresolved variables as random noise terms.

141 Many stochastic parameterizations are based on the assumption of a scale separation between
142 the temporal decorrelation rates between the rapidly fluctuating processes represented by a
143 white noise and the slow processes of interest (e.g., Gardiner, 1985; Penland, 2003a). In
144 geophysical applications, there is often - but not always – a relationship between spatial and
145 temporal scales of variability, with fast processes associated with small scales and slow
146 processes associated with large scales. If this is the case, separating physical processes by
147 timescales can result in decomposing small-scale features from large-scale phenomena and
148 spatial and temporal scale separation become equivalent.

149 Such a thinking underlies the pioneering study of Hasselmann (1976), who split the coupled
150 ocean-atmosphere system into a slow ocean and fast weather fluctuation components and
151 subsequently derived an effective equation for the ocean circulation only. One finds that the
152 impact of the fast variables on the dynamics of the slow variables boils down to a
153 deterministic correction – a mean field effect sometimes referred to as noise-induced drift
154 or rectification – plus a stochastic component, which is a white random noise in the limit of
155 infinite time scale separation.

156 A simple example demonstrating noise-induced transitions and drifts is presented in Figure
157 1. Assume, the unforced nonlinear climate system can be described by a double-well
158 potential (a). If the noise is sufficiently small (denoted by short red arrows) and under
159 appropriate initial conditions, the system will stay in the deeper potential well and the
160 associated probability density function of states will have a single maximum (b). As the
161 amplitude of the noise increases (long arrows in c), the system can undergo a noise-induced
162 transition and reach the secondary potential well. The resulting probability density function
163 (PDF) will exhibit two local maxima (d), signifying two different climate regimes, rather
164 than a single maximum, as in the small-noise scenario. Note, that the stochastic forcing not
165 only changes the variance, but also the mean.

166 But even a linear system characterized by a single potential when unforced can change the
167 mean, if forced by multiplicative or state-dependent white noise (e-h). The noise is called
168 “multiplicative”, if its amplitude is a function of the state, which is denoted by the red errors of
169 different length in panel g. The noise-induced drift changes the single-well potential of the
170 unforced system (e), so that the effective potential including the effects of the multiplicative
171 noise has multiple wells (not shown) and the associated PDF becomes bimodal (h). Note, that in
172 this example the shift in the mean compared to the unforced PDF (f) is caused by the noise,
173 which is referred to as “noise-induced drift” (see e.g., Sardeshmukh et al. 2001, Berner 2005,
174 Berner et al. 2005, Sura et al. 2005).

175 Operational weather and climate centers use now stochastic parameterization schemes routinely
176 to make ensemble predictions from short-range to seasonal time scales (e.g., Berner et al. 2009,
177 Weisheimer et al. 2014). Most ensembles suffer from underdispersion, which means that - on
178 average – the observed state is more often outside the cone of forecasts than can be statistically

179 justified. Stochastic perturbations introduce more diversity among the forecasts, which helps to
180 ameliorate this problem and result in more skillful ensemble forecasts.

181 A fundamental argument, that has been often overlooked, is that the merit of stochastic
182 parameterization goes far beyond providing uncertainty estimations for weather and climate
183 predictions, but may be also needed for better representing the mean state (e.g., Sardeshmukh et
184 al. 2001, Palmer 2001, Berner et al. 2008) and regime transitions (e.g., Williams et al. 2003,
185 2004, Birner and Williams 2008, Christensen et al. 2015a) via inherent non-linear processes.
186 This is especially relevant for climate projections, which have long-standing mean state errors,
187 such as e.g., a double inter-tropical convergence zone (e.g., Lin et al. 2007), and erroneous
188 stratocumulus cloud cover, which play a crucial role in the climate response to external forcing.

189 Mechanisms for how Gaussian zero-mean fluctuations can change the mean state (see Figure 1)
190 have been discussed e.g. in Tompkins and Berner (2008) and Beena and von Storch (2009).

191 Tompkins and Berner (2008) introduce perturbations to the humidity field and find that positive
192 perturbations are more likely to trigger a convective event than negative perturbations can
193 suppress convection. Beena and von Storch (2009) study the ocean response air-sea flux
194 perturbations and similarly find that negative buoyancy anomalies result in an altered
195 stratification, while positive anomalies tend to sustain the existing stratification. Insofar as
196 stochastic parameterizations can change the mean state, they have the potential to affect the
197 response to changes in the external forcing (e.g., Seiffert and von Storch 2008).

198 In mathematical terms, this is the question how a stochastic forcing affects the invariant measure
199 of a deterministic dynamical system (Lucarini 2012) and how the climate response to such a
200 forcing can be framed as a problem of non-equilibrium statistical mechanics (Colangeli et al.
201 2012, 2014, Lucarini and Sarno 2011, Lucarini et 2014a,b).

202 Here, we argue, that stochastic parameterizations are essential for:

- 203 • Estimating uncertainty in weather and climate predictions
- 204 • Reducing systematic model errors arising from unrepresented subgrid-scale fluctuations
- 205 • Triggering noise-induced regime transitions
- 206 • Capturing the response to changes in the external forcing

207 and should be applied in a systematic and consistent fashion, not only to weather, but also to
208 climate simulations.

209 Several studies have identified the assessment of the benefits of stochastic closure schemes as
210 key outstanding challenge in the area of mathematics applied to the climate system (Palmer
211 2001, 2012, Palmer and Williams 2008, Williams et al. 2013). For accessible reviews of
212 rigorous mathematical approaches applied to weather and climate, we refer to Penland
213 (2003a,b), Majda et al. (2008) and Franzke et al. (2015). The current study focuses on recent
214 developments and successful applications of empirical and rigorous approaches to the subgrid-
215 parameterization problem in weather and climate models.

216 **2 Representing Uncertainty in Comprehensive Climate and Weather Models**

217 *2.1 Adding uncertainty a posteriori: the stochastically perturbed parameterization tendency* 218 *scheme and the stochastic kinetic-energy backscatter scheme*

219 Stochastic parameterizations are based on the notion that – as spatial resolution increases – the
220 method of averaging (Arnold 2001, Monahan and Culina 2011) is no longer valid and the
221 subgrid-scale variability should be sampled rather than represented by the equilibrium mean. In
222 addition, unrepresented interactions between unresolved subgrid-scale processes with the large-

223 scale flow might affect the resolved dynamics.

224 Former is addressed by the stochastically perturbed parameterization tendency (SPPT) scheme,
225 which perturbs the net tendencies of the physical process parameterizations (convection,
226 radiation, cloud physics, turbulence and gravity wave drag). One essential feature for its success
227 is that the noise is correlated in space and time. SPPT has a beneficial impact on medium range,
228 seasonal and climate forecasts (Buizza et al. 1999, Teixeira and Reynolds 2008, Palmer et al.
229 2009, Weisheimer et al. 2014, Christensen et al. 2015b, Dawson and Palmer 2015, Batté and
230 Doblus-Reyes 2015). SPPT tends to be most active in the tropics and near the surface, where
231 the parameterized tendencies are large.

232 The stochastic kinetic-energy backscatter scheme (SKEBS) aims to represent model uncertainty
233 arising from unresolved subgrid-scale processes and their interactions with larger scales by
234 introducing random perturbations to the streamfunction and potential temperature tendencies.
235 For this purpose, the scheme re-injects a small fraction of the dissipated energy into the resolved
236 flow. Originally developed in the context of Large Eddy Simulations (LES; Mason and
237 Thomson 1992), it was adapted by Shutts (2005) for Numerical Weather Prediction (NWP).

238 Depending on the details of the implementations, SKEBS tends to have most impact in the
239 storm-track regions and in the free atmosphere above the boundary layer and permits the
240 physical parameterization schemes to adjust to a slightly perturbed large-scale background flow.
241 Its beneficial impact on weather and climate forecasts are reported e.g., in Berner et al. (2011,
242 2015), Tennant et al. (2011), Weisheimer et al. (2014), Sanchez et al. (2015); albeit Shutts
243 (2013) criticizes the arbitrary nature of some of the design features based on coarse-graining
244 high-resolution simulations to compute the backscatter term. His stochastic convective
245 backscatter scheme (Shutts, 2015) includes a phase relationship between flow and perturbations

246 and adds additional perturbations to the divergent flow to remedy some of the identified
247 shortcomings.

248 While these schemes are motivated by physical reasoning and scheme parameters are
249 informed in some manner, for example by coarse-graining high-resolution output (Shutts
250 and Palmer 2007, Shutts and Callado Pallarès 2014) or comparison with observations
251 (Watson et al. 2015), the perturbations are essentially empirical constructs. For example,
252 the amplitude of the perturbations is typically determined as the value that satisfactorily
253 reduces the ensemble underdispersion. Obviously such an approach is only possible for
254 forecast ranges where verification is possible, such as for short-term, medium-range and
255 seasonal forecasts. A common criticism of this approach is that the improved skill is solely
256 the result of the increase in spread. However, Berner et al. (2015) found that the merits of
257 stochastic parameterization go beyond increasing spread and can account for structural
258 model uncertainty.

259 In the following examples, we show recent results that demonstrate the potential of
260 stochastic parameterizations to improve the mean state representation and variability as
261 well as the skill of seasonal forecasts.

262 First, we present recent results from the seasonal forecasting system at ECMWF. In the
263 simulations with both, SPPT and SKEBS, excessively strong convective activity over the
264 Maritime Continent and the tropical Western Pacific is reduced, leading to smaller biases in
265 outgoing longwave radiation (Figure 2, adapted from Weisheimer et al. 2014), cloud cover,
266 precipitation and near-surface winds. The stochastic schemes also lead to an increase in the
267 frequency (Figure 3, from Weisheimer et al. 2014) and amplitude of MJO events, which is

268 an improvement. A reduction of excessive amplitudes in westward propagating
269 convectively coupled waves in an earlier model version is reported in Berner et al. 2012.

270 Another example of the positive impact of stochastic schemes is evident in climate
271 simulations with the Community Earth System Model (CESM). Compared to observations,
272 the modeled spectrum of average sea surface temperature in the Nino 3.4 region has three
273 times more power for periods between 2 and 4 years (Figure 4, adapted from Christensen et
274 al. 2016). SPPT markedly reduces the temperature variability in this frequency range,
275 leading to a much better agreement with nature (Christensen et al., 2016). Interestingly, in
276 these examples adding stochasticity results in *reduced* variability, which is a non-trivial
277 response.

278 Along with the improved model climate, stochastic perturbations benefit probabilistic
279 forecast performance on seasonal timescales. This has been reported in a number of studies
280 using earlier versions of ECMWF's seasonal system (Berner et al. 2008, Dobles-Reyes et
281 al. 2009, Palmer et al. 2009) and recently been confirmed in the newest version
282 (Weisheimer et al. 2014) and in the EC-Earth system model (Batté and Doblas-Reyes
283 2015). Figure 5 shows ensemble mean and spread in forecasts for Nino 3.4 area sea-surface
284 temperatures with the EC-Earth model, run at a standard horizontal resolution (SR, ca.
285 60km for the atmospheric and ca. 100km for the ocean component) and a high resolution
286 (HR, ca. 40km for the atmospheric component and 25km for the ocean.) For both
287 resolutions, the introduction of SPPT perturbations increases the ensemble spread.
288 Furthermore, SPPT reduces the mean error in the standard resolution, but not as much as
289 increasing horizontal resolution.

290 A number of studies have found evidence for stochasticity leading to noise-induced
291 transitions in mid-latitude circulation regimes, especially over the Pacific-North America
292 region (Jung et al. 2005, Berner et al. 2012, Dawson et al. 2015, Weisheimer et al. 2014).
293 These results suggest that stochastic parameterizations are also relevant for the prediction of
294 the dominant modes of atmospheric variability such as the North Atlantic Oscillation and
295 the Pacific North American pattern (Berner et al. 2016).

296 ***2.2 Adding uncertainty a priori: perturbed parameter approaches for the atmospheric*** 297 ***component***

298 While the performance of the stochastic schemes discussed in the last section is undisputed,
299 they have been criticized in that they are added *a posteriori* to models that have been
300 independently developed and tuned. Ideally, stochastic perturbations should represent
301 model uncertainty where it occurs. One obvious way to represent uncertainty at its source
302 rather than *a posteriori* is the perturbed parameter approach, which perturbs the closure
303 parameters in the physical process parameterizations. There are two variants: the parameter
304 can be fixed throughout the integration, but vary for each ensemble member (e.g. Murphy
305 et al. 2004, Hacker et al. 2011a) or vary randomly with time (e.g. Bowler et al. 2008, 2009,
306 Ollinaho et al. 2013, Jankov et al., 2016). Strictly, the first variant is not a stochastic
307 parameterization, but an example for a multi-model, since each ensemble member has a
308 different climatology. However, since stochastic parameter perturbations are routinely
309 compared to fixed-parameter schemes, this section discusses both.

310 While perturbed-parameter ensembles typically outperform unperturbed ensembles on
311 weather timescales, they typically cannot sufficiently account for all deficiencies in the
312 spread (Hacker et al. 2011, Reynolds et al. 2011, Christensen et al. 2015b) and do not lead

313 to the same reliability as the *a posteriori* schemes discussed above (Berner et al., 2015).
314 Presumably, this is due to the fact that *a posteriori* schemes are designed to
315 encapsulate all model uncertainty, of which parameter uncertainty is only one
316 contributor.

317 An ensemble system is considered statistically reliable when a predicted probability for a
318 particular event (e.g. temperature exceeding 17°C) compares well with the observed
319 frequencies. Another limitation of this approach is that the parameter uncertainty estimates
320 are subjective, and information about parameter interdependencies is not included.

321 The following studies are examples for applications of the perturbed-parameter approach to
322 physical process parameterizations and perturbing the interface between different model
323 components. We start with results pertaining to perturbations in the atmospheric
324 component and move to those of other model components, such as land and ocean models,
325 which are more relevant for climate applications.

326 A number of studies report on improved skill due to parameter perturbations to boundary
327 layer and convection schemes (Hacker et al. 2011, Reynolds et al. 2011, Jankov et al.,
328 2016). Recently, a stochastic "eddy-diffusivity/ mass-flux" parameterization has been
329 developed (Suselj et al. 2014), which combines an eddy-diffusivity component with a
330 stochastic mass-flux scheme. The resulting scheme unifies boundary layer and shallow
331 convection and was operationally implemented in the operational Navy Global
332 Environmental Model.

333 Christensen et al. (2015b) used an objective covariance estimate of parameter uncertainty
334 (Järvinen et al. 2012, Ollinaho et al. 2013) for four convection closure parameters and developed

335 both a fixed-parameter and a stochastically varying perturbation scheme. Both schemes
336 improved the forecast skill of the ECMWF ensemble prediction system, with a larger impact
337 observed for the fixed perturbed parameter scheme (Figure 6, adapted from Christensen et al.
338 2015b). In addition, for some variables such as wind at 850hPa, the scheme leads to a reduction
339 in bias (Figure 6, adapted from Christensen et al. 2015b).

340 Recently, a body of work proposes stochastic approaches for another atmospheric
341 parameterization, namely non-orographic gravity waves (Lott et al. 2012, Lott and Guez 2013,
342 and de la Cámara and Lott 2015). Observational studies indicate that the gravity wave field is
343 very intermittent and only predictable in a statistical sense. Recently, de la Cámara et al. (2014)
344 informed the free parameters of the stochastic gravity-wave scheme using momentum flux
345 measurements.

346 *2.3 Uncertainty in land surface, ocean and coupled component models*

347 Physical parameters of land surface models are often not well constrained by observations. A
348 recent study by MacLeod et al. (2015) introduced parameter perturbations to key soil
349 parameters, and compared their impact with stochastic perturbations of the soil moisture
350 tendencies in seasonal forecasts with the ECMWF coupled model. Both the perturbed parameter
351 approach and the stochastic tendency perturbations improved the forecasts of extreme air
352 temperature for the European heat wave of 2003.

353 A shortcoming in land models stems from the omission of sub-grid land heterogeneity, which
354 impacts the surface heat flux. Langan et al. (2014) retained the subgrid-variability by drawing
355 the area for each plant functional types at each timestep from a Dirichlet distribution, rather than
356 using constant area weights. First results with a single column model version of CESM reveal an
357 increase in the variability as well as larger extreme values in convective precipitation (Figure 7,

358 adapted from by Langan et al. 2014).

359 The coupled atmosphere-ocean system is very sensitive to fluctuations in the fluxes between its
360 component models. Air-sea fluxes of buoyancy, energy, and momentum vary on a vast range of
361 space and time scales, including scales that are too small or fast to be explicitly resolved by
362 global climate models. For example, convective clouds in the atmosphere will cause subgrid
363 fluctuations at the air-sea interface, in both, the downward fresh water flux and short-wave solar
364 radiation. The response of the climate to stochastic perturbations of the air-sea buoyancy flux is
365 studied by Williams (2012) in a coupled atmosphere-ocean model. The response is complex and
366 involves changes to the oceanic mixed-layer depth, sea-surface temperature, atmospheric Hadley
367 circulation, and fresh water flux across the sea surface (Figure 8, from Williams 2012). These
368 findings suggest that the lack of representation of stochastic subgrid variability in air-sea fluxes
369 may contribute to some of the biases exhibited by contemporary coupled climate models.

370 Since the buoyancy effects in the ocean are different from that in the atmosphere, the length
371 scale at which rotational effects become as important as gravity wave effects is much smaller.
372 Consequently, mesoscale eddies in state-of-the art ocean models are still far from being resolved
373 and are usually represented by traditional bulk parameterizations (Gent and McWilliams 1990,
374 Redi 1982). A recent study by Li and von Storch (2013) computes the contributions from the
375 mean and fluctuating component of heat flux divergence in a high-resolution ocean model. The
376 magnitude of the fluctuations is about one order of magnitude larger than the mean component
377 (Figure 9, adapted from Li and von Storch 2013) suggesting that classical parameterizations
378 significantly underestimate the total eddy flux. The fluctuating part, even though having zero
379 mean, can play an important role in generating large-scale low-frequency variations and in
380 shaping the mean oceanic circulation.

381 Juricke et al. (2013) and Juricke and Jung (2014) recently investigated the sensitivity of an
382 ocean-sea ice model to variations in the ice strength parameter. As this parameter is not
383 observable, large uncertainties remain in the choice of its value, although it is very important for
384 modeling sea ice drift. Varying this parameter stochastically results in changes to the mean sea
385 ice distribution as well as sea ice spread. Compared to perturbations of the atmospheric initial
386 conditions, the incorporation of additional stochastic ice strength perturbations leads to a
387 considerably increase in spread of the simulated sea ice thickness in the central Arctic
388 (Figure 10, adapted from Juricke et al. 2014), which is a better match with the observed
389 uncertainties (Juricke et al. 2014).

390 *2.4 Data Assimilation and Extreme Events*

391 The purpose of data assimilation is to combine observations with short-term model-forecasts to
392 come up with a gridded and physically consistent estimate of the state of the atmosphere, also
393 called “analysis”. One method is to use short-term forecasts as the first guess fields in ensemble
394 data assimilation. As such, ensemble data assimilation inherits the shortcomings of short-term
395 ensemble predictions, namely, the underdispersiveness in the spread. Recent work has
396 demonstrated that the stochastic parameterizations that are beneficial for ensemble prediction,
397 can also improve analyses fields (Isaksen et al. 2007, Houtekamer et al. 2009, Mitchell and
398 Gottwald 2012, Hamill and Whitaker 2011, Ha et al. 2015, Romine et al. 2015). In particular,
399 Ha et al. 2015 showed that the inclusion of a stochastic parameterization improved the mean
400 analysis, even if the observations were constrained to those in the control experiment. A cutting-
401 edge frontier is the use of memory effects in Kalman filter data assimilation schemes (O’Kane
402 and Frederiksen 2012).

403 The impact of stochastic perturbations on extremes has only been considered very recently. A

404 body of work focuses on the description of non-Gaussian subgrid-scale processes (Majda et al.
405 2009, Sardeshmukh and Sura 2009, Sura 2011, Sardeshmukh et al. 2015). Franzke (2012)
406 showed that his reduced stochastic model (see next section) captures the extremes of the full
407 model. He et al. (2012) studied the influence of an explicitly stochastic representation of mixing
408 in the stable boundary layer on the extremes of near-surface wind speed in a single column
409 model. Tagle et al. (2015) were the first to study the effect of the stochastic parameterizations in
410 a comprehensive climate model. They found that the stochastic parameterizations had a big
411 impact on the surface temperature mean and variability, but hardly changed the tail behavior.

412 **3 Systematic mathematical and statistical physics approaches**

413 This section introduces systematic mathematical and statistical physics approaches to the
414 parameterization problem and reports on recent work on the application of these rigorous
415 methods to the weather and climate system.

416 ***3.1. Mathematical and Numerical implications of stochasticity***

417 Although the motions of the atmosphere and ocean are described by the Navier-Stokes
418 equation, large-scale flows can often be modeled under hydrostatic approximation. This
419 leads to the deterministic primitive equation system. If we want to represent continuous
420 small-scale fluctuations as stochastic terms, these equations need to be generalized to allow
421 for stochasticity. A relevant mathematical field is thus the extension of the derivation to the
422 stochastic primitive equations for two-dimensional (Ewald et al. 2007; Glatt-Holtz and
423 Ziane 2008; Glatt-Holtz and Temam 2011) and three-dimensional flows (Debussche et al.
424 2012).

425 Moreover, stochastic systems require calculi and numerical schemes fundamentally
426 different from the ones available to solve deterministic systems. The two most commonly
427 used stochastic integral types are the Itô-integral (Itô 1951) and the Stratonovich-integral
428 (Stratonovich 1966). When the fast processes of a continuous system are modeled by white
429 noise – as is common for physical applications - the resulting stochastic model converges to
430 a Stratonovich stochastic differential equation (Wong and Zakai 1965, Papanicolaou and
431 Kohler 1974, Gardiner 1985, Penland 2003a,b). Discrete systems converge to the Itô
432 stochastic differential equation. Starting in the 1970s a solid framework of numerical
433 methods for stochastic ordinary differential equations was developed (Rümelin 1982,
434 Kloeden and Platen 1992, Milstein 1995, Kloeden 2002). However, this has been extended
435 to high-order schemes only recently (Jentzen and Kloeden 2009, Weniger 2014). With
436 stochastic parameterizations becoming more common in weather and climate simulations, a
437 revision of the deterministic numerical schemes should be undertaken to ensure the
438 convergence of the numerical solutions.

439 *3.2 Homogenization and stochastic mode reduction*

440 Numerical weather and climate modeling can be seen as a model reduction problem. Because
441 we cannot numerically solve the full continuous equations, we have to truncate the equations at
442 some scale and then treat the unresolved processes in some smart way. A systematic approach
443 for the derivation of reduced order models from first principles is performed through the method
444 of homogenization or adiabatic elimination (Wong and Zakai 1965, Khas'minskii 1966, Kurtz
445 1973, Papanicolaou and Kohler 1974, Pavliotis and Stuart 2008). The fundamental idea is to
446 decompose the state vector into slow and fast components, represent the fast processes by a
447 stochastic term and derive analytically an effective equation for the slow, predictable modes.

448 Majda et al. (1999) and Majda et al., 2001 expanded this body of work by making additional
449 assumptions on the nonlinear self-interaction of the fast modes and coined the term “stochastic
450 mode reduction”.

451 The stochastic mode reduction has been demonstrated to successfully model regime-behavior
452 and low-frequency variability for conceptual models of the atmosphere (Majda et al. 2003), the
453 barotropic vorticity (Franzke et al. 2005) and a quasi-geostrophic three-layer model on the
454 sphere with realistic orography (Franzke and Majda 2006). However, due to both, the sheer
455 amount of analytical derivation and the compute-memory requirement in the numerical
456 implementation of the resulting equations, the stochastic mode reduction cannot be easily
457 applied to comprehensive climate models of arbitrary complexity. A possible way forward is to
458 apply the stochastic mode reduction locally at each gridpoint rather than globally (Dolaptchiev
459 et al. (2013 a,b).

460 These mathematical techniques are rigorously valid only in the limit of large time-scale
461 separation, although some studies report good empirical results, even when this condition is not,
462 or only partly met (Dozier and Tappert 1978a,b , Majda et al. 2003 2008, Franzke et al. 2005,
463 Franzke and Majda 2006). When the time scale separation between the fast and slow processes
464 is not too large, the picture of the parameterization as being constructed as the sum of a suitably
465 defined deterministic plus random corrections has to be amended to take memory effects into
466 account (e.g. Zwanzig 2001, Chekroun et al. 2015a,b). Unfortunately, the condition of scale
467 separation is typically not met in geophysical fluid dynamics applications (Sardeshmukh and
468 Penland 2015, Yano 2015, Yano et al. 2015), which poses limitations to the application of
469 homogenization. An alternative, which does not make any assumptions about time scale
470 separation and provides an explicit expression for the terms responsible for the memory effect is

471 proposed by Wouters and Lucarini (2012, 2013), who, instead, assume the presence of a weak
472 dynamical coupling between the fast and the slow scales of motion.

473 The question of which stochastic process is best suited to describe the nonlinear interactions of
474 the unresolved processes is an open topic. While methods for Gaussian diffusion processes are
475 well known (Oppenheim 1975) it may be the case that other formulations like Lévy processes
476 are better suited to describe the underlying physics. For the interested reader, we refer to recent
477 studies by Penland and Ewald 2008, Penland and Sardeshmukh 2012, Hein et al. 2010, Gairing
478 and Imkeller 2012, 2013, Thompson et al. 2015.

479 *3.3 Adaptation of Concepts from Statistical Physics to Weather and Climate*

480 The scale-aware representation of convection and clouds on high-resolution grids (1-50
481 km) has been a long-standing challenge for weather and climate models. Within a single
482 model column, convection is not uniquely determined by the resolved-scale processes,
483 and the distribution of possible realizations of subgrid-scale convection highly depends on
484 model resolution. Furthermore, horizontal transports of heat, moisture or momentum
485 from neighboring grid-boxes are typically neglected. Thus, to achieve scale-awareness, it
486 is necessary to represent scale-dependent convective fluctuations about the ensemble
487 average response. In addition, because of the lack of time-scale separation, a correct
488 representation of convection across scales requires memory of subgrid-states from
489 previous time steps.

490 A novel approach to represent the fluctuations in an ensemble of deep convective clouds adapts
491 concepts from statistical mechanics (Craig and Cohen 2006). Based on this theory, a stochastic
492 parameterization of deep convection was developed to represent fluctuations of the subgrid

493 convective mass flux about statistical equilibrium (Plant and Craig 2008). This is especially
494 attractive for variable-resolution grids, since the statistics automatically adapt to the grid-
495 resolution. This approach was extended to shallow convective clouds by introducing a memory
496 effect arising from the correlation between the cloud mass fluxes and cloud lifetimes (Sakradzija
497 et al. 2015). Figure 11 (adapted from Sakradzija et al. 2015) shows histograms of the subgrid
498 cloud-base mass flux in the stochastic shallow cumulus cloud scheme and coarse-grained large-
499 eddy simulation at different horizontal resolutions. The histograms match closely and are scale-
500 aware.

501 ***3.4 Modeling convective processes by Markov chains and cellular automata***

502 Another way to introduce temporal memory and nonlocal effects is the use of Markov
503 chains and cellular automata. A Markov chain is a mathematical system that undergoes
504 transitions from one *discrete* state to another and the probabilities associated with the
505 various state changes are called transition probabilities. If observational data or high-
506 resolutions simulations are used to inform the transition probabilities, the Markov chains
507 are called data-driven.

508 An example for this approach is the “stochastic convective parameterization” which
509 describes the convective state of the entire model column as a discrete Markov chain.
510 (Khouider et al. 2010, Dorrestijn et al. 2013a,b, 2015, Gottwald et al. 2015). The system
511 can only reside in a few distinct convective states – e.g., but not necessarily: clear sky,
512 shallow or deep convection, - and the random transitions from one state to another evolve
513 as a Markov chain. For example, Dorrestijn et al. 2013a cover the horizontal domain of the
514 numerical model with a high-resolution lattice (with typical lattice spacing of 100m to
515 1000m), and on each lattice node lives a copy of the discrete stochastic process for the

516 convective state (Figure 12, adapted from Dorrestijn et al. 2013a). The transition
517 probabilities are estimated from a cloud-resolving LES model. By averaging over blocks of
518 lattice nodes, convective area fractions and related quantities can be obtained for spatial
519 domains of arbitrary size. The resulting patterns and temporal behavior of the area fractions
520 are quite realistic. Furthermore, the formulation on a high-resolution lattice (or microlattice)
521 makes it possible to compute convective fractions for varying area sizes, so that a
522 parameterization based on these fractions is scale-adaptive.

523 Frenkel et al. (2012) and Peters et al. (2013) use the stochastic model introduced in
524 Khouider et al. (2010), but different methods to estimate the transition probabilities.
525 Khouider et al (2010) and Frenkel et al. (2012) formulate the rules based on physical
526 insight, while Peters et al. (2013) use observations for their estimates. Latter find that the
527 estimates from observation can notably differ from those based on physical intuition.

528 A related approach are cellular automata which are often used as simple mathematical
529 models to simulate spatial self-organizational behavior such as convective organization A
530 cellular automaton describes the evolution of discrete states on a lattice grid. The states are
531 updated according to a set of rules based on the states of neighboring cells at the previous
532 time step. In addition to memory, cellular automata can allow for lateral communications
533 between neighboring grid boxes and thus introduce spatial correlations.

534 The idea of using cellular automata within NWP was first proposed by Palmer (2001) and
535 first applications used them as a quasi-stochastic pattern generator for SKEBS (Shutts 2005,
536 Berner et al. 2008). Bengtsson et al. (2013) pioneered the use of a cellular automaton for
537 the parameterization of convection, which allows for the horizontal transports of heat,
538 moisture and momentum across neighboring grid-boxes. The scheme has been shown to

539 enhance the organization of convective squall-lines (Bengtsson et al. 2013) and improves
540 the skill of accumulated precipitation in a high-resolution ensemble prediction system
541 (Bengtsson and Körnich 2015).

542 *3.5 Climate Response in the presence of small-scale fluctuations*

543 While there is extensive work focusing on the response of the climate system to changes in
544 the external forcing, either natural - such as the forcing from a localized tropical heating as
545 it occurs in Nino - or anthropogenic - such from increased greenhouse gases, little attention
546 has been given to the fact if and how the representation of the subgrid-scale can alter that
547 response. In the mathematical community, this is the topic of response theory and the
548 fluctuation-dissipation theorem (e.g., Marconi et al. 2008, Lacorata and Vulpiani 2007,
549 Colangeli et al. 2011, Lucarini and Colangeli 2012, Colangeli and Lucarini 2014).

550 Seiffert and von Storch (2008) were the first to investigate the response of a climate model
551 to CO₂-forcing in the presence of subgrid-scale fluctuations in atmospheric temperature,
552 divergence and vorticity. In their model, the strength of the global warming due to a CO₂-
553 doubling is altered by up to 15% near the surface and up to 25% in the upper troposphere
554 (Figure 13, from Seiffert and von Storch 2008) depending on the exact representation of the
555 small-scale fluctuations. Applying a stochastic model to their simulations, they found that
556 the small-scale fluctuations change the temperature response via a statistical damping
557 that acts as a restoring force. In addition, the small-scale fluctuations can affect feedback
558 and interaction processes that are directly coupled to an increase in CO₂, thereby altering
559 the CO₂-related radiative forcing (Seiffert and von Storch 2010).

560 The fluctuation-dissipation theorem (FDT) is concerned with the response of a system to
561 small changes in the forcing. In particular, it tries to relate the response to the natural

562 fluctuations in the system (Kubo 1966, Deker and Haake 1975, Hänggi and Thomas 1977,
563 Leith 1975, Risken 1984). In the atmospheric sciences, the FDT-operator is estimated from
564 model output, in particular the variances and covariances of the state variables at different
565 time lags. The so obtained empirical linear model is able to predict the response to changes
566 in the external forcing, such as signature from localized tropical heat forcing (Gritsun and
567 Branstator 2007, Gritsun et al. 2008).

568 Achatz et al. (2013) argue that subgrid-scale parameterizations developed for a present day
569 climate, might no longer be accurate in a changing climate. They use the FDT to adjust the
570 subgrid-scale representation of the forced system. Figure 14 (adapted from Achatz et al.
571 2013) shows that a low-order model with a subgrid-scale parameterization corrected by the
572 FDT yields a better response in streamfunction variance than without the correction.

573 While some success of FDT-techniques to low-frequency climate modeling has been
574 demonstrated, some of the mathematical assumptions are not strictly met. Recent work expands
575 the mathematical underpinning by formulating the response theory more generally and is better
576 suited for non-equilibrium systems (Ruelle 2009, Lucarini and Sarno 2011) and climate
577 projections (Lucarini et al. 2014, Ragone et al. 2015).

578 ***3.6 Statistical Dynamical Closure Theory***

579 Kraichnan (1959) first illustrated that renormalization of the statistical equations of fluid
580 motion can be used to produce self-consistent parameterizations of the subgrid turbulent
581 processes. It is on this basis that Frederiksen and Davies (1997) developed stochastic
582 parameterisations of subgrid turbulence in barotropic atmospheric simulations on the
583 sphere. The subgrid parameterizations consist of drain, backscatter and net eddy viscosities,
584 which are determined from the statistics of higher resolution closure simulations. The aim

585 here is that the spectra from the low-resolution simulation with stochastic subgrid
586 parameterization should be ideally statistically indistinguishable from those produced by
587 the high-resolution simulation, which would allow to save computational resources.
588 Implementation of this approach into an atmospheric GCM resulted in significantly
589 improved circulation and energy spectra (Frederiksen et al. 2003). These ideas were further
590 developed by Frederiksen (1999, 2012a,b), and O’Kane and Frederiksen (2008).
591 Frederiksen and Kepert (2006) then used the functional form of these closure approaches to
592 develop a zero-parameter stochastic modeling framework, where the eddy viscosities are
593 determined from higher-resolution reference simulations. This approach was successfully
594 applied to baroclinic geophysical simulations in Zidikheri and Frederiksen (2009, 2010a,b).
595 Recently, Kitsios et al. (2012, 2013,2014) used this approach to determine the eddy
596 viscosities from a series of high-resolution atmospheric and oceanic reference simulations.
597 The isotropized versions of the subgrid-eddy viscosities were then characterized by a set of
598 scaling laws. Large eddy simulations with subgrid models defined by these scaling laws
599 (solid lines in Figure 15) were able to reproduce the statistics of the high-resolution
600 reference simulations (dashed lines in Figure 15) across all resolved scales. This
601 demonstrates that including a stochastic subgrid parameterization in the low-resolution
602 simulations makes them indistinguishable from the high-resolution reference.
603 The scaling laws further enable the subgrid parameterizations to be utilized more widely, as
604 they remove the need to generate the subgrid coefficients from a reference simulation.

605 **Concluding Remarks**

606 In this article, we attempt to narrow the gap between the fields of numerical meteorological
607 models and applied mathematics in the development of stochastic parameterizations: on the one

608 hand geo-scientists are often unaware of mathematically rigorous results that can aid in the
609 development of physically relevant parameterizations, on the other hand mathematicians often
610 do not know about open issues in scientific applications that might be mathematically tractable.
611 Over the last decade or two, increasing evidence has pointed to the potential of this
612 approach, albeit applied in an *ad hoc* manner and tuned to specific applications. This is
613 apparent in the choices made at operational weather centers, where stochastic
614 parameterization schemes are now routinely used to represent model inadequacy better and
615 improve probabilistic forecast skill. Here, we revisit recent work that demonstrates that
616 stochastic parameterizations are not only essential for the estimation of the uncertainty in
617 weather forecasts, but are also necessary for accurate climate and climate change
618 projections. Stochastic parameterizations have the potential to reduce systematic model
619 errors, trigger noise-induced regime transitions, and modify the response to changes in the
620 external forcing.

621 Ideally, stochastic parameterizations should be developed alongside the physical
622 parameterization and dynamical core development and not tuned to yield a particular model
623 performance. This approach is hampered by the fact that parameters in climate and weather
624 are typically adjusted (“tuned”) to yield the best mean state and/or the best variability. This
625 can result in compensating model errors, which pose a big challenge to model development
626 in general, and stochastic parameterizations in particular. A stochastic parameterization
627 might improve the model from a process perspective, but its decreased systematic error no
628 longer compensates other model errors, resulting in an overall larger bias (Palmer and
629 Weisheimer 2011, Berner et al. 2012). Clearly, such structural uncertainties need to be
630 addressed in order to improve the predictive skills of our models.

631 Mathematically rigorous approaches decompose the system-at-hand into slow and fast
632 components. They focus on the accurate simulation of the large, predictable scales, while only
633 the statistical properties of the small, unpredictable scales need to be captured. One finds that the
634 impact of the fast variables on the dynamics of the slow variables boils down to a deterministic
635 correction plus a stochastic component. This immediately points to the fact that the classical
636 parameterization approach, which is only based upon averaged properties, is insufficient.
637 Understanding the deterministic correction term in physical terms will shed light on the impact
638 of stochastic parameterizations on systematic model errors and, hopefully, compensating model
639 errors.

640 Recent findings from such rigorous derivations suggest that when the time scales of the
641 processes we need to parameterize are not very different from those of the explicitly resolved
642 dynamics – if we are in a grey zone - memory terms can become important. This is especially
643 relevant for developing scale-aware parameterizations, where it is difficult to control the time
644 scale separation as the spatial resolution is altered.

645 Of course, the stochastic approach is not a panacea for the subgrid-scale parameterization
646 problem and persistent model biases. Stochastic approaches must complement
647 developments in the deterministic physical process parameterizations and dynamical core,
648 as motivated e.g. by Stevens and Bony (2013) and Jakob (2014). Nevertheless, it is our
649 conviction, that basing stochastic parameterizations on sound mathematical and statistical
650 physics concepts will lead to substantial improvements in our understanding of the Earth
651 system as well as increased predictive capability in next generation weather and climate
652 models.

653 **Acknowledgements**

654 The idea for this article was conceived at the workshop on “Stochastic
655 Parameterisation in Weather and Climate Models” held at the Meteorological Institute,
656 University of Bonn, Germany, September 16-19, 2013. We thank the Meteorological
657 Institute for hosting the workshop and the VolkswagenStiftung for financial support
658 (Ref: 86951). We thank Dr. Karsten Peters and two anonymous reviewers as well as
659 the editor Dr. Brian Etherton for insightful and detailed suggestions, which greatly
660 improved the manuscript. Thanks also to Drs. Hugh Morrison and Wojciech Grabowski
661 for thoughtful comments on an earlier version of the manuscript.

662 REFERENCES

- 663 Achatz, U., U. Löbl, S. I. Dolaptchiev, and A. Gritsun, 2013: Fluctuation–dissipation
664 supplemented by nonlinearity: A climate-dependent subgrid-scale parameterization in low-order
665 climate models. *J. Atmos. Sci.*, **70**, 1833–1846.
- 666 Arakawa, A., 2004: The Cumulus Parameterization Problem: Past, Present, and Future. *J.*
667 *Climate*, **17**, 2493–2525.
- 668 Arnold, L., 2001: Hasselmann's program revisited: the analysis of stochasticity in deterministic
669 climate models. In *Stochastic Climate Models*, Birkhäuser, Imkeller and von Storch, eds. Pp.
670 141-157.
- 671 Batté L. and Doblas-Reyes, 2015: Stochastic atmospheric perturbations in the EC-Earth3
672 global coupled model: impact of SPPT on seasonal forecast quality *Climate Dynamics*
673 45:3419–3439. DOI 10.1007/s00382-015-2548-7
- 674 Bauer, P., Thorpe, A., and Brunet, G., 2015: The quiet revolution of numerical weather
675 prediction. *Nature*, **525**, 47-55.
- 676 Bengtsson, L., M. Steinheimer, P. Bechtold, and J.-F. Geleyn, 2013: A stochastic
677 parametrization for deep convection using cellular automata, *Quarterly Journal of the Royal*
678 *Meteorological Society*, **139**, 1533-1543
- 679 Bengtsson, L., Körnich, H., 2015: Impact of a stochastic parameterization of cumulus
680 convection, using cellular automata, in a meso-scale ensemble prediction system. *Quarterly*
681 *Journal of the Royal Meteorological Society*. DOI: 10.1002/qj.2720
- 682 Beena, B. S. and J.-S. Von Storch, 2009: Effects of fluctuating daily surface fluxes on the
683 time- mean oceanic circulation. *Climate dynamics*, **33**, 1–18.
- 684 Berner, J , H. Christensen and D. Coleman, 2016: “Impact of stochastic parametrization in
685 the Earth System Community Model”, to be submitted to *J. Clim.*
- 686 Berner, J., F. J. Doblas-Reyes, T. N. Palmer, G. Shutts, and A. Weisheimer, 2008: Impact
687 of a quasi-stochastic cellular automaton back- scatter scheme on the systematic error and
688 seasonal prediction skill of a global climate model. *Philos. Trans. Roy. Soc. London*, **366A**,
689 2561–2579.
- 690 Berner, J., 2005: Linking nonlinearity and non-Gaussianity of planetary wave behavior by
691 the Fokker–Planck equation. *J. Atmos. Sci.*, **62**, 2098–2117.
- 692 Berner, J., and G. Branstator, 2007: Linear and nonlinear signatures in the planetary wave
693 dynamics of an AGCM: Probability Density Functions. *J. Atmos. Sci.*, **64**, 117–136.
- 694 Berner, J., S.-Y. Ha, J. P. Hacker, A. Fournier, and C. Snyder, 2011: Model uncertainty in a
695 mesoscale ensemble prediction system: Stochastic versus multi-physics representations.
696 *Mon. Wea. Rev.*, **139**, 1972–1995.
- 697 Berner, J, T. Jung, and T. N. Palmer, 2012: Systematic model error: The impact of
698 increased horizontal resolution versus improved stochastic and deterministic
699 parameterizations. *J. Climate*, **25**, 4946–4962.

700 Berner, J., K. R. Smith, S.-Y. Ha, J. Hacker and C. Snyder, 2015: Increasing the skill of
701 probabilistic forecasts: Understanding performance improvements from model-error
702 representations, *Mon. Wea. Rev.*, 143, 1295–1320.

703 Birner, T. and Williams, P. D., 2008: Sudden stratospheric warmings as noise-induced
704 transition. *J. Atmos. Sci.*, 65(10), 3337–3343.

705 Buizza, Roberto, M. Miller, and T. N. Palmer, 1999: Stochastic representation of model
706 uncertainties in the ECMWF ensemble prediction system. *QJR Meteorol. Soc.*, 125, 2887–
707 2908.

708 Bowler N.E., A. Arribas, K.R. Mylne, K. B. Robertson, S.E. Beare, 2008: The MOGREPS
709 short-range ensemble prediction system. *Q. J. R. Meteorol. Soc.*, 134, 703 – 722

710 Bowler, N. E., A. Arribas, S. E. Beare, K. R. Mylne, and G. J. Shutts, 2009. The local
711 ETKF and SKEB: Upgrades to the MOGREPS short-range ensemble prediction
712 system. *QJR Meteorol. Soc.*, 135, 767–776.

713 de la Cámara, A., F. Lott, and A. Hertzog, 2014: Intermittency in a stochastic
714 parameterization of nonorographic gravity waves, *J. Geophys. Res. Atmos.*, 119, 11,905–
715 11,919, doi:10.1002/2014JD022002.

716 de la Cámara, A., and F. Lott, 2015: A parameterization of gravity waves emitted by fronts
717 and jets, *Geophys. Res. Lett.*, 42, 2071–2078, doi:10.1002/2015GL063298.

718 Charron, M., G. Pellerin, L. Spacek, P. L. Houtekamer, N. Gagnon, H. L. Mitchell, and L.
719 Michelin, 2010: Toward random sampling of model error in the Canadian Ensemble
720 Prediction System. *Mon. Wea. Rev.*, 138, 1877–1901.

721 Chekroun, M., Liu, H., and Wang, S., 2015: Approximation of Stochastic Invariant
722 Manifolds: Stochastic Manifolds for Nonlinear SPDEs I, Springer Briefs in Mathematics

723 Chekroun, M., Liu, H., and Wang, S., 2015: Approximation of Stochastic Invariant
724 Manifolds: Stochastic Manifolds for Nonlinear SPDEs II, Springer Briefs in Mathematics

725 Crommelin, Daan, and Eric Vanden-Eijnden, 2008: Subgrid-scale parameterization with
726 conditional Markov chains. *J. Atmos. Sci.* 65.8: 2661–2675.

727 Christensen, H., J. Berner, D. Coleman and T. N. Palmer, 2016: “Stochastic parametrisation
728 and the El Nino-Southern Oscillation”, submitted to *J. Clim.*

729 Christensen, H. M., Moroz, I. M. and Palmer, T. N., 2015a: Simulating weather regimes:
730 impact of stochastic and perturbed parameter schemes in a simple atmospheric model.
731 *Climate Dynamics* 44, 2195–2214.

732 Christensen, H. M., Moroz, I.M., Palmer, T.N., 2015b: Stochastic and perturbed parameter
733 representations of model uncertainty in convection parameterization. *J. Atmos. Sci.*, 72, 2525–
734 2544.

735 Colangeli, M., L. Rondoni and A. Verderosa, 2014: Focus on some nonequilibrium issues,
736 *Chaos, Solitons & Fractals* 64, 2

737 Colangeli, M., L. Rondoni, A. Vulpiani, 2012: Fluctuation-dissipation relation for chaotic
738 non-Hamiltonian systems, *J. Stat. Mech.: Theor. Exp.* L04002

739 Colangeli, M., C. Maes and B. Wynants, 2011: A meaningful expansion around detailed
740 balance, *J.Phys. A: Math. Theor.* 44, 095001.

741 Colangeli M. and V. Lucarini, 2014: Elements of a unified framework for response
742 formulae, *J. Stat.Mech.: Theor. Exp.* P01002

743 Craig, G. C. and B. G. Cohen, 2006: Fluctuations in an equilibrium convective ensemble, part I:
744 Theoretical formulation. *J. Atmos. Sci.*, 63, 1996–2004.

745 Dawson, A. and T. N. Palmer, 2015: Simulating weather regimes: Impact of model
746 resolution and stochastic parameterization. *Climate Dynamics*, 44, 2177–2193.

747 Debussche, A., N. Glatt-Holtz, R. Temam, and M. Ziane, 2012: Global Existence and Regularity
748 for the 3D Stochastic Primitive Equations of the Ocean and Atmosphere with Multiplicative
749 White Noise. *Nonlinearity*, 25.

750 Deker, U., and F. Haake, 1975: Fluctuation-dissipation theorems for classical processes.
751 *Phys. Rev.*, 11A, 2043–2056

752 Doblas-Reyes, F. J., et al. 2009: Addressing model uncertainty in seasonal and annual
753 dynamical ensemble forecasts. *Q.J.R. Meteorol. Soc.*, 135.643, 1538–1559.

754 Dolaptchiev, S., U. Achatz, and I. Timofeyev, 2013a: Stochastic closure for local averages in the
755 finite-difference discretization of the forced burgers equation. *Theoretical and Computational
756 Fluid Dynamics*, 27, 297–317.

757 Dolaptchiev, S. I., I. Timofeyev, and U. Achatz, 2013b: Subgrid-scale closure for the inviscid
758 Burgers-Hopf equation. *Commun. Math. Sci.*, 11, 757–777.

759 Dorfman, J. R., 1999: *An introduction to chaos in nonequilibrium statistical mechanics* (No.
760 14). Cambridge University Press.

761 Dorrestijn, J., Crommelin, D. T., Biello, J. A., and Böing, S. J., 2013a: A data-driven multi-
762 cloud model for stochastic parametrization of deep convection. *Philosophical Transactions
763 of the Royal Society A: Mathematical, Physical and Engineering Sciences* , 371, 20120374.

764 Dorrestijn, J., D. T. Crommelin, A. P. Siebesma, and H. J.J. Jonker, 2013b: Stochastic
765 parameterization of shallow cumulus convection estimated from high-resolution model
766 data, *Theoretical and Computational Fluid Dynamics*, 27

767 Dorrestijn, J., D. T. Crommelin, A. P. Siebesma, H. J.J. Jonker and C. Jakob, 2015:
768 Stochastic parameterization of convective area fractions with a multcloud model inferred
769 from observational data. *J. Atmos. Sci.*, 72, 854–869.

770 Dozier, L.B., and F.D. Tappert, 1978a: Statistics of normal mode amplitudes in a random
771 ocean. I. Theory. *J. Acoust. Soc. Am.*, **63**, 353–365.

772 Dozier, L.B., and F.D. Tappert, 1978b: Statistics of normal mode amplitudes in a random
773 ocean. II. Computations. *J. Acoust. Soc. Am.*, **64**, 533–547.

774 Español, P., 1998: Stochastic differential equations for non-linear hydrodynamics, *Physica
775 A*, 248, 77–96.

776 Eckermann, S. D., 2011: Explicitly stochastic parameterization of nonorographic gravity
777 wave drag, *J. Atmos. Sci.*, 68, 1749—1765.

778 Ewald, B., M. Petcu, and R. Temam, 2007: Stochastic Solutions of the Two-Dimensional
779 Primitive Equations of the Ocean and Atmosphere with an Additive Noise. *Analysis and*
780 *Applications*, 5, 183.

781 Franzke C., 2012: Predictability of extreme events in a non-linear stochastic-dynamical
782 model. *Phys Rev E*, 85, doi: 10.1103/PhysRevE.85.031134.

783 Franzke, C. and A. J. Majda, 2006: Low-order stochastic mode reduction for a prototype
784 atmospheric GCM. *J. Atmos. Sci.*, 63, 457–479.

785 Franzke, C., A. J. Majda, and E. Vanden-Eijnden, 2005: Low-order stochastic mode reduction
786 for a realistic barotropic model climate. *J. Atmos. Sci.*, 62, 1722–1745.

787 Franzke, C. L., T. J. O’Kane, J. Berner, P. D. Williams, and V. Lucarini, 2015: Stochastic
788 climate theory and modeling. *Wiley Interdisciplinary Reviews: Climate Change*, 6, 63–78.

789 Frederiksen, J. S., 1999: Subgrid-scale parameterizations of eddy-topographic force, eddy
790 viscosity and stochastic backscatter for flow over topography. *J. Atmos. Sci.*, 56, 1481–1493.

791 Frederiksen, J. S. 2012a: Self-energy closure for inhomogeneous turbulence and subgrid
792 modeling. *Entropy*, 14, 769–799.

793 Frederiksen, J. S. 2012b: Statistical dynamical closures and subgrid modeling for
794 inhomogeneous QG and 3D turbulence. *Entropy*, 14, 32–57.

795 Frederiksen, J. S. and A. G. Davies, 1997: Eddy viscosity and stochastic backscatter
796 parameterizations on the sphere for atmospheric circulation models. *J. Atmos. Sci.*, 54, 2475–
797 2492.

798 Frederiksen, J. S., M. R. Dix, and A. G. Davies, 2003: The effects of closure-based eddy
799 diffusion on the climate and spectra of a GCM. *Tellus*, 55, 31–44.

800 Frederiksen, J. S., M. R. Dix, and S. M. Kepert, 1996: Systematic energy errors and tendency
801 toward canonical equilibrium in atmospheric circulation models. *J. Atmos. Sci.*, 53, 887–904.

802 Frederiksen, J. S. and S. M. Kepert, 2006: Dynamical subgrid-scale parameterizations from
803 direct numerical simulations. *J. Atmos. Sci.*, 63, 3006–3019.

804 Frenkel, Yevgeniy, Andrew J. Majda, and Boualem Khouider. 2012: Using the stochastic
805 multcloud model to improve tropical convective parameterization: A paradigm example. *J.*
806 *Atmos. Sci.*, 69, 1080–1105.

807 Gairing, J. and P. Imkeller, 2012: Power variations of heavy tailed jump diffusions in
808 paleoclimatic time series. *EGU General Assembly Conference Abstracts*, volume 14, 11612.

809 Gairing, J. M. and P. Imkeller, 2013: Stable clts and rates for power variation of α -stable Levy
810 processes. *Methodology and Computing in Applied Probability*, 1–18.

811 García, A.L., and C. Penland, 1991: Fluctuating Hydrodynamics and Principal Oscillation
812 Pattern Analysis, *J. Stat. Phys.*, 64, 1121–1132.

813 Gardiner, C. W., 1985: *Handbook of Stochastic Methods for Physics, Chemistry and the Natural*
814 *Sciences*. Springer Verlag, Berlin Heidelberg New York, 442 pp.

815 Gent, Peter R., and James C. McWilliams. Isopycnal mixing in ocean circulation
816 models. *Journal of Physical Oceanography* 20.1 (1990): 150–155.

817 Gerard, L. 2007: An integrated package for subgrid convection, clouds and precipitation
818 compatible with meso-gamma scales. *Quart. J. Roy. Meteor. Soc.* 133, 711–730.

819 Gaspard, P. 2005: *Chaos, scattering and statistical mechanics* (Vol. 9). Cambridge
820 University Press.

821 Glatt-Holtz, N. and R. Temam, 2011: Pathwise Solutions of the 2-D Stochastic Primitive
822 Equations. *Applied Mathematics & Optimization*, 63, 401–433.

823 Glatt-Holtz, N. and M. Ziane, 2008: The Stochastic Primitive Equations in Two Space
824 Dimensions with Multiplicative Noise. *Discrete Contin. Dyn. Syst. Ser. B*, 10, 801–822.

825 Gottwald, G.A., K. Peters and L. Davies (2015), A data-driven method for the stochastic
826 parametrisation of subgrid-scale tropical convective area fraction. *Q.J.R. Meteorol. Soc.*, DOI:
827 10.1002/qj.2655

828 Gritsun, A. S, and G. Branstator, 2007: Climate response using a three-dimensional operator
829 based on the fluctuation–dissipation theorem. *J. Atmos. Sci.*, 64, 2558–2575.

830 Gritsun, A. S, Branstator, G., and A. Majda, 2008: Climate response of linear and quadratic
831 functionals using the fluctuation–dissipation theorem. *J. Atmos. Sci.*, 65, 2824–2841

832 Ha, S.-Y., J. Berner, and C. Snyder, 2014: Model error representation in mesoscale WRF-
833 dart cycling. *Monthly Weather Review* 2015, doi: [http://dx.doi.org/10.1175/MWR-D-14-](http://dx.doi.org/10.1175/MWR-D-14-00395.1)
834 [00395.1](http://dx.doi.org/10.1175/MWR-D-14-00395.1)

835 Hacker JP, Snyder C, Ha S-Y, Pocerlich M (2011) Linear and non-linear response to parameter
836 variations in a mesoscale model. *Tellus*, 63A, 429–444, doi: 10.1111/j.1600-0870.2010.00505.x.

837 Houtekamer, P. L., H. L. Mitchell and X. Deng, 2009: Model error representation in an
838 operational ensemble Kalman filter. *Mon. Wea. Rev.*, 137, 2126–2143,
839 doi:10.1175/2008MWR2737.1

840 Hänggi, P., and H. Thomas, 1977: Time evolution, correlations and linear response of non-
841 Markov processes. *Z. Phys.*, 26B, 85–92.

842 Hasselmann, K., 1976: Stochastic Climate Models. Part I: Theory. *Tellus*, 28, 473–485.

843 He, Y., A. H. Monahan, and N. A. McFarlane, 2012: The influence of boundary layer
844 processes on the diurnal variation of the climatological near-surface wind speed probability
845 distribution over land. *J. Climate*, 25, 6441–6458.

846 Hein, C., P. Imkeller, and I. Pavlyukevich, 2010: Limit theorems for p-variations of solutions of
847 SDES driven by additive stable Lévy noise and model selection for paleo-climatic data. *Recent*
848 *Development in Stochastic Dynamics and Stochastic Analysis*, 8, 137–150.

849 Horsthemke, W. and R. Lefever, 1984: *Noise-induced transitions*. Springer Verlag, Berlin
850 Heidelberg New York, 318 pp.

851 Hung, M.-P., Lin, J.-L., Wang, W., Kim, D., Shinoda, T. and Weaver, S.J. 2013: MJO and
852 convectively coupled equatorial waves simulated by CMIP5 climate models. *Journal of Climate*
853 26: 6185–6214

854 Itô, K., 1944: Stochastic integral. *Proceedings of the Imperial Academy*, 20, 519–524,
855 doi:10.3792/pia/1195572786. URL <http://dx.doi.org/10.3792/pia/1195572786> Itô, K., 1951: On

856 Stochastic Differential Equations. *American Mathematical Society, New York*, 4, 1–51.

857 Jankov I., J. Berner, J. Beck, G. Grell, J. Olson, G. Grell, 2016: Performance Comparison Between
858 Multi-Physics and Stochastic Approaches Within a North American RAP Ensemble, *Mon. Wea. Rev.*,
859 submitted

860 Jakob, C. (2014), Going back to basics, *Nature Clim. Change*, 4, 1042–1045,
861 doi:10.1038/nclimate2445

862 Järvinen H, Laine M, Solonen A, Haario H (2012) Ensemble prediction and parameter
863 estimation system: The concept. *Q. J. R. Meteorol. Soc.*, 138, 281 – 288. doi:
864 10.1002/qj.923.

865 Jentzen, A. and P. E. Kloeden, 2009: The Numerical Approximation of Stochastic Partial
866 Differential Equations. *Milan J. Math.*, vol. 77 no. 1, 205–244, doi:10.1007/s00032-009-0100-0.

867 Jung, Thomas, T. N. Palmer, and G. J. Shutts. Influence of a stochastic parameterization on
868 the frequency of occurrence of North Pacific weather regimes in the ECMWF
869 model. *Geophysical research letters* 32.23 (2005).

870 Juricke, S. and T. Jung, 2014: Influence of stochastic sea ice parameterization on climate and the
871 role of atmosphere-sea ice-ocean interaction. *Phil. Trans. R. Soc. A*, 372, 20130283

872 Juricke, S., H. F. Goessling, and T. Jung, 2014: Potential sea ice predictability and the role of
873 stochastic sea ice strength perturbations. *Geophys. Res. Lett.*, 41, 8396–8403,

874 Juricke, S., P. Lemke, R. Timmermann, and T. Rackow, 2013: Effects of stochastic ice strength
875 perturbation on arctic finite element sea ice modeling. *Journal of Climate*, 26.

876 Khas'minskii, R. Z., 1966: A limit theorem for the solutions of differential equations with
877 random right-hand sides. *Theory Prob. and App.*, 11, 390-406.

878 Khouider, B., J. Biello, and A. J. Majda, 2010: A stochastic multcloud model for tropical
879 convection. *Communications in Mathematical Sciences*, 8, 187-216.

880 Kitsios, V., J. S. Frederiksen, and M. J. Zidikheri, 2012: Subgrid model with scaling laws for
881 atmospheric simulations. *J. Atmos. Sci.*, 69, 1427–1445.

882 Kitsios, V., J. S. Frederiksen, and M. J. Zidikheri, 2013: Scaling laws for parameterisations of
883 subgrid eddy-eddy interactions in simulations of oceanic circulations. *Ocean Modelling*, 68, 88–
884 105.

885 Kitsios, Vassili, J. S. Frederiksen, and M. J. Zidikheri, 2014: Scaling laws for parametrizations of
886 subgrid interactions in simulations of oceanic circulations. *Philosophical Transactions of the
887 Royal Society of London A: Mathematical, Physical and Engineering Sciences* 372.2018:
888 20130285. .

889 Kloeden, P. E., 2002: The systematic derivation of higher order numerical schemes for
890 stochastic differential equations. *Milan Journal of Mathematics*, 70, 187–207.

891 Kloeden, P. E. and E. Platen, 1992: *Numerical Solutions of Stochastic Differential Equation*.
892 Springer Verlag, Berlin, 636 pp.

893 Kraichnan R. H, 1959: The structure of isotropic turbulence at very high Reynolds number.
894 *J Fluid Mech.*, 5, 497-543.

- 895 Kubo, R., 1966: The fluctuation-dissipation theorem, *Rep. Prog. Phys.*, 29, 255-284.
- 896 Kurtz, T. G., 1973: A limit theorem for perturbed operator semi-groups with applications to
897 random evolutions. *J. Funct. Anal.*, 12, 55–67.
- 898 Lacorata, G. A. Vulpiani., 2007: Fluctuation-Response Relation and modeling in systems with
899 fast and slow dynamics, *Nonlin. Processes Geophys.*, 14, 681–694
- 900 Landau, L.D., and E.M. Lifshitz, 1959: *Fluid Mechanics*, Pergamon Press.
- 901 Leith, C. E, 1975: Climate response and fluctuation dissipation. *J. Atmos. Sci.* 32, 2022-2026
- 902 Li, H. and J.-S. von Storch, 2013: On the fluctuations of buoyancy fluxes simulated in a 1/10
903 degree ogcm. *J. Phys. Oceanogr.*, 43.
- 904 Lin, J.L., 2007: The Double-ITCZ Problem in IPCC AR4 Coupled GCMs: Ocean–
905 Atmosphere Feedback Analysis. *J. Climate*, 20, 4497–4525.
- 906 Langan, R., Archibald, R., Plumlee, M., Mahajan, S., Ricciuto, D., Yang, C., ... and Fu, J.
907 S. (2014). Stochastic Parameterization to Represent Variability and Extremes in Climate
908 Modeling. *Procedia Computer Science*, 29, 1146-1155.
- 909 Lott, F., L. Guez, and P. Maury, 2012: A stochastic parameterization of non-orographic
910 gravity waves: Formalism and impact on the equatorial stratosphere, *Geophys. Res. Lett.*,
911 39, L06807, doi:10.1029/2012GL051001.
- 912 Lott, F., and L. Guez, 2013: A stochastic parameterization of the gravity waves due to
913 convection and its impact on the equatorial stratosphere, *J. Geophys. Res. Atmos.*, 118,
914 8897-8909, doi:10.1002/jgrd.50705.
- 915 Louis, J.-F., 1979: A parametric model of vertical eddy fluxes in the atmosphere. *Bound.-*
916 *Layer Meteor.*, 17, 1876-202, doi 10.1007/BF00117978.
- 917 Lucarini, V., 2012: Stochastic perturbations to a dynamical system: a response theory approach,
918 *J. Stat. Phys.* 146, 774-786
- 919 Lucarini, V and M. Colangeli, 2012: Beyond the Fluctuation-Dissipation Theorem: The role
920 of Causality, *J. Stat. Mech.: Theor. Exp.* P05013
- 921 Lucarini, V. and S Sarno, 2011: A statistical mechanical approach for the computation of the
922 climatic response to general forcings. *Nonlinear Processes in Geophysics*, 18, 7-28
- 923 Lucarini, V., Faranda, D., Wouters, J., and Kuna, T. 2014a Towards a General Theory of
924 Extremes for Observables of Chaotic Dynamical Systems. *J. Stat. Phys.* 154, 723-750.
- 925 Lucarini, V., R Blender, C Herbert, F Ragone, S Pascale, J Wouters, 2014b: Mathematical
926 and physical ideas for climate science, *Reviews of Geophysics* 52 (4), 809-859
- 927 Majda, A.J., Gershgorin, B., and Y. Yuan, 2010: Low frequency climate response and
928 fluctuation–dissipation theorems: Theory and practice. *J. Atmos. Sci.*, 67, 1186–1201.
- 929 MacLeod, D., H. L. Cloke, F. Pappenberger and A. Weisheimer (2015): Improved seasonal
930 prediction of the hot summer of 2003 over Europe through better representation of uncertainty in
931 the land. *Q. J. R. Meteorol. Soc.*, doi:10.1002/qj.2631.
- 932 Majda, A. J, C. Franzke and D. Crommelin, 2009: Normal forms for reduced stochastic climate

933 models. *Proc. Natl. Acad. Sci. USA*, doi:10.1073/pnas.0900173106.

934 Majda, A. J., C. Franzke, and Boualem Khouider, 2008: An applied mathematics
935 perspective on stochastic modelling for climate. *Philosophical Transactions of the Royal
936 Society of London A: Mathematical, Physical and Engineering Sciences* 366.1875: 2427-
937 2453.

938 Majda, A., I. Timofeyev, and E. Vanden-Eijnden, 2003: Systematic strategies for stochastic
939 mode reduction in climate. *J. Atmos. Sci.*, 60, 1705–1722.

940 Majda, A. J., I. Timofeyev, and Vanden-Eijnden, 1999: Models for Stochastic Climate
941 Prediction. *Proc. Natl Acad. Sci. USA*, 96, 14687–14691.

942 Majda, A. J., I. Timofeyev, and Vanden-Eijnden, 2001: A Mathematical Framework for
943 Stochastic Climate Models. *Commun. Pure Appl. Math.*, 54, 891–974.

944 Marconi, U.M.B, A. Puglisi, L. Rondoni, A. Vulpiani, 2008: Fluctuation–dissipation:
945 Response theory in statistical physics, *Physics Reports* 461, 111–195.

946 Mason, P. J. and Thomson, D. J., 1992: Stochastic backscatter in large-eddy simulations of
947 boundary layers. *Journal of Fluid Mechanics*, 242, 51-78.

948 Milstein, G. N., 1995: *Numerical integration of stochastic differential equations*, volume 313.
949 Springer.

950 Mitchell L, Gottwald GA. Data assimilation in slow-fast systems using homogenized
951 climate models. *J Atmos Sci* 2012, 69:1359–1377.

952 Monahan, A., and J. Culina, 2011: Stochastic averaging of idealized climate models. *J.
953 Climate*, 24, 3068-3088.

954 O’Kane, T. J. and J. S. Frederiksen, 2008: Statistical dynamical subgrid-scale parameterizations
955 for geophysical flows. *Phys. Scr.*, T132, 014033.

956 O’Kane T.J., Frederiksen J.S., 2012: The application of statistical dynamical turbulence
957 closures to data assimilation. *Phys. Scr.*, T142, 014042.

958 Ollinaho P, Laine M, Solonen A Haario H, Järvinen H (2013) NWP model forecast skill
959 optimization via closure parameter variations. *Q. J. R. Meteorol. Soc.*, 139, 1520 – 1532.
960 doi: 10.1002/qj.2044.

961 Oppenheim, A., 1975: Schafer rw: Digital signal processing. *Englewood Clifis, N.J.: Prentice-
962 Hall*.

963 Palmer, T. N. 2012, Towards the probabilistic Earth-system simulator: a vision for the future of
964 climate and weather prediction. *Q.J.R. Meteorol. Soc.*, 138: 841–861. doi: 10.1002/qj.1923

965 Palmer, T. N., 2001: A nonlinear dynamical perspective on model error: A proposal for non-
966 local stochastic-dynamic parameterization in weather and climate prediction. *Quart. J. Roy.
967 Meteor. Soc.*, 127, 279–304.

968 Palmer, T. N., R. Buizza, F. Doblas-Reyes, T. Jung, M. Leutbecher, G. Shutts, M. Steinheimer,
969 and A. Weisheimer, 2009: Stochastic Parametrization and Model Uncertainty. *ECMWF
970 Technical Memorandum*, 598, available at <http://www.ecmwf.int/publications/>.

- 971 Palmer, T. N., and A. Weisheimer, 2011. Diagnosing the causes of bias in climate models–
972 why is it so hard? *Geophysical & Astrophysical Fluid Dynamics* 105.2-3, 351-365.
- 973 Palmer, T. N. and Williams, P. D., 2008: Introduction. Stochastic physics and climate
974 modeling. *Philosophical Transactions of the Royal Society A*, 366, 2421-2427.
- 975 Papanicolaou, G., and W. Kohler, 1974: Asymptotic theory of mixing ordinary stochastic
976 differential equations. *Comm. Pure Appl. Math.*, **27**, 641-668.
- 977 Pavliotis, G. A. and A. M. Stuart, 2008: Multiscale methods, volume 53 of Texts in Applied
978 Mathematics, Springer, New York, NY
- 979 Penland, C., 2003a: Noise out of chaos and why it won't go away. *Bull. Amer. Meteor. Soc.*, 84,
980 921–925.
- 981 Penland, C., 2003b: A stochastic approach to nonlinear dynamics: A review (electronic
982 supplement to 'noise out of chaos and why it won't go away'). *Bull. Amer. Meteor. Soc.*, 84,
983 ES43–ES51.
- 984 Penland, C. and B. Ewald, 2008: On Modelling Physical Systems with Stochastic Models:
985 Diffusion versus Lévy Processes. *Philosophical Transactions of the Royal Society A:*
986 *Mathematical, Physical and Engineering Sciences*, 366, 2455–2474.
- 987 Penland, C. and P. D. Sardeshmukh, 2012: Alternative interpretations of power-law distributions
988 found in nature. *Chaos: An Interdisciplinary Journal of Nonlinear Science*, 22, 023119.
- 989 Peters, K., Jakob, C., Davies, L., Khouider, B., & Majda, A. J. (2013). Stochastic behavior
990 of tropical convection in observations and a multcloud model. *J. Atmos. Sci.*, 70, 3556-
991 3575.
- 992 Plant, R. S. and G. C. Craig, 2008: A stochastic parameterization for deep convection based on
993 equilibrium statistics. *J. Atmos. Sci.*, 65, 87–105.
- 994 Ragone, F., V. Lucarini, F. Lunkeit, 2015: A new framework for climate sensitivity and
995 response: a modeling perspective, *Clim. Dyn.*, doi: 10.1007/s00382-015-2657-3
- 996 Redi, M. H., 1982: Oceanic isopycnal mixing by coordinate rotation. *JPO*, 12, 1154-1158
- 997 Reynolds CA, Ridout JA, McLay JG, 2011: Examination of parameter variations in the
998 U.S. Navy global ensemble. *Tellus*, 63A, 841 – 857.
- 999 Risken, H., 1984: The Fokker-Plank Equation: Methods of Solution and Applications. Springer-
1000 Verlag, 474 pp.
- 1001 Ruelle, D., 2009: A review of linear response theory for general differentiable dynamical
1002 systems. *Nonlinearity*, **22**, 855-870.
- 1003 Ruelle, D., 2012: Hydrodynamic turbulence as a problem in nonequilibrium statistical
1004 mechanics. *PNAS*, **109**, 20344-20346.
- 1005 Ruelle., D., 2014: Non-equilibrium statistical mechanics of turbulence. *J. Stat. Phys.*, **157**, 205-
1006 218.
- 1007 Romine, G. S., C. S. Schwartz, J. Berner, K. R. Smith, C. Snyder, J. L. Anderson, and M. L.
1008 Weisman, 2014: Representing forecast error in a convection-permitting ensemble system.
1009 *Mon. Wea. Rev.*, **142**, 4519–4541.

- 1010 Rümelin, W., 1982: Numerical Treatment of Stochastic Differential Equations. *SIAM J.*
1011 *Numer. Anal.*, **19**, 604-613.
- 1012 Sakradzija, M., A. Seifert, and T. Heus, 2015: Fluctuations in a quasi-stationary shallow
1013 cumulus cloud ensemble. *Nonlin. Processes Geophys.*, **22**, 65-85.
- 1014 Sanchez, C., Williams, K. D. and Collins, M. (2015), Improved stochastic physics schemes for
1015 global weather and climate models. Q.J.R. Meteorol. Soc.. doi: 10.1002/qj.2640
- 1016 Sardeshmukh, P., C. Penland, and M. Newman, 2001: *Rossby waves in a fluctuating medium.*
1017 *Progress In Probability, Vol 49: Stochastic Climate Models*. P. Imkeller, and J.-S. von Storch,
1018 eds., Birkäuser Verlag, Basel, 369–384, 369–384 pp.
- 1019 Sardeshmukh, P.D., and P. Sura 2009: Reconciling non-Gaussian climate statistics with linear
1020 dynamics. *J. Climate*, **22**, 1193-1207.
- 1021 Sardeshmukh, P.D., and C. Penland, 2015: Understanding the distinctively skewed and
1022 heavy tailed character of atmospheric and oceanic probability distributions. *Chaos*, **25**,
1023 036410, doi: 10.1063/1.4914169
- 1024 Sardeshmulh, P.D., G.P. Compo, and C. Penland, 2015: Need for caution in interpreting extreme
1025 weather statistics. *J. Climate*, doi: <http://dx.doi.org/10.1175/JCLI-D-15-0020.1>.
- 1026 Schumacher, J., J.D. Scheel, D. Krasnov, D.A.Donzis, V. Yakhot, and K.R. Sreenivasan, 2014:
1027 Small-scale universality in fluid turbulence. *PNAS*, 10961-10965.
- 1028 Seiffert, R., and J-S. Von Storch, 2008: Impact of atmospheric small-scale fluctuations on
1029 climate sensitivity." *Geophysical Research Letters*, 35.10.
- 1030 Seiffert, R. and J.-S. von Storch, 2010: A stochastic analysis of the impact of small-scale
1031 fluctuations on tropospheric temperature response to CO2 doubling. *J. Climate*, 23, 2307-
1032 2319.
- 1033 Shutts, G., 2015, A stochastic convective backscatter scheme for use in ensemble prediction
1034 systems. Q.J.R. Meteorol. Soc., doi: 10.1002/qj.2547
- 1035 Shutts, G, 2005: A kinetic energy backscatter algorithm for use in ensemble prediction systems.
1036 *Quarterly Journal of the Royal Meteorological Society*, 3079-3102.
- 1037 Shutts, G. J., 2013. Coarse graining the vorticity equation in the ECMWF integrated
1038 forecasting system: The search for kinetic energy backscatter. *Journal of the Atmospheric*
1039 *Sciences*, 70(4), 1233-1241.
- 1040 Shutts, G., T. Allen, and J. Berner, 2008: Stochastic parameterization of multiscale processes
1041 using a dual-grid approach. *Philosophical Transactions of the Royal Society A: Mathematical,*
1042 *Physical and Engineering Sciences*, 366, 2623–2639.
- 1043 Shutts, G. J., and T. N. Palmer, 2007: Convective forcing fluctuations in a cloud-resolving
1044 model: Relevance to the stochastic parameterization problem. *Journal of climate*, 20, 187-
1045 202.
- 1046 Shutts, G. and A. Callado Pallarès, 2014: Assessing parameterization uncertainty associated
1047 with horizontal resolution in numerical weather prediction models. *Philosophical*
1048 *Transactions of the Royal Society of London A: Mathematical, Physical and Engineering*
1049 *Sciences* 372.2018, 20130284.

- 1050 Stevens, B., and S. Bony (2013), What Are Climate Models Missing?, *Science*, 340 (6136),
1051 1053–1054, doi:10.1126/science.1237554.
- 1052 Stratonovich, R., 1966: A new representation for stochastic integrals and equations. *SIAM*
1053 *Journal on Control*, 4, 362–371.
- 1054 Sura P., 2011: A general perspective of extreme events in weather and climate. *Atmos. Res.*,
1055 101, 1–21.
- 1056 Sura, P., M. Newman, C. Penland, and P. Sardeshmukh, 2005: Multiplicative noise and
1057 non-Gaussianity: A paradigm for atmospheric regimes? *J. Atmos. Sci.*, 62, 1391-1409.
- 1058 Suselj, K., J. Teixeira, D. Chung, 2013: A Unified Model for moist-convective boundary
1059 layers based on a stochastic eddy-diffusivity/ mass-flux parameterization. *J. Atmos. Sci.*, **70**,
1060 1929-1953.
- 1061 Suselj, K., T.F. Hogan, J. Teixeira, 2015: Implementation of a stochastic eddy-diffusivity/
1062 mass flux parameterization into the Navy Global Environmental Model. *Weather and*
1063 *Forecasting*, **29**, 1374-1390.
- 1064 Tagle, F., J. Berner, M. D. Grigoriu, N. M. Mahowald, G. Samorodnitsky, 2015:
1065 Temperature Extremes in the Community Atmosphere Model with Model Error
1066 Representation, *J. Clim*, doi: <http://dx.doi.org/10.1175/JCLI-D-15-0314.1>
- 1067 Tennant, W.J., et al, 2011: Using a stochastic kinetic energy backscatter scheme to
1068 improve MOGREPS probabilistic forecast skill , *Monthly Weather Review*, 139, 1190-1206.
- 1069 Teixeira J., and C. Reynolds, 2008: Stochastic nature of physical parameterizations in
1070 ensemble prediction: A stochastic convection approach . *Mon. Wea. Rev.*, 136, 483–496.
- 1071 Thompson, W.F., R.A. Kuske, A.H. Monahan, 2015: Stochastic averaging of dynamical
1072 systems with multiple time scales forced with a-stable noise. *Multiscale Interactions*, in
1073 press.
- 1074 Tompkins, A. M., and J. Berner, 2008: A stochastic convective approach to account for
1075 model uncertainty due to unresolved humidity variability. *Journal of Geophysical*
1076 *Research: Atmospheres* 113.D18
- 1077 Watson, P. A. G., H. M. Christensen, and T. N. Palmer, 2015: Does the ECMWF IFS
1078 Convection Parameterization with Stochastic Physics Correctly Reproduce Relationships
1079 between Convection and the Large-Scale State? *J. Atmos. Sci.*, 72(1), 236–242.
- 1080 Weniger, M., 2014: Stochastic Parameterization: A Rigorous Approach to Stochastic Three-
1081 Dimensional Primitive Equations. *Bonner Meteorologische Abhandlungen*, 64.
- 1082 Weisheimer, A., S. Corti, T.N. Palmer and F. Vitart (2014): Addressing model error
1083 through atmospheric stochastic physical parameterisations: Impact on the coupled ECMWF
1084 seasonal forecasting system. *Phil. Trans. R. Soc. A* , **372**, 201820130290, doi:
1085 10.1098/rsta.2013.0290
- 1086 Weisheimer, A., T. N. Palmer, and F. J. Doblas-Reyes. 2011: Assessment of
1087 representations of model uncertainty in monthly and seasonal forecast
1088 ensembles. *Geophysical Research Letters* 38.16 (2011).

1089 Williams, P. D., Read, P. L. and Haine, T. W. N., 2003: Spontaneous generation and impact
1090 of inertia–gravity waves in a stratified, two-layer shear flow. *Geophysical Research Letters*,
1091 30(24), article number 2255.

1092 Williams, P. D., Haine, T. W. N. and Read, P. L., 2004: Stochastic resonance in a nonlinear
1093 model of a rotating, stratified shear flow, with a simple stochastic inertia–gravity wave
1094 parameterization. *Nonlinear Processes in Geophysics*, 11(1), 127-135.

1095 Williams, P. D., 2005: Modelling climate change: the role of unresolved processes.
1096 *Philosophical Transactions of the Royal Society A*, 363(1837), 2931-2946.

1097 Williams, P. D., 2012: Climatic impacts of stochastic fluctuations in air–sea fluxes. *Geophysical
1098 Research Letters*, 39, article number L10705.

1099 Williams, P. D., Cullen, M. J. P., Davey, M. K. and Huthnance, J. M., 2013: Mathematics
1100 applied to the climate system: outstanding challenges and recent progress. *Philosophical
1101 Transactions of the Royal Society A*, 371(1991), article number 20120518.

1102 Wouters, J. and V. Lucarini, 2012: Disentangling multi-level systems: averaging, correlations
1103 and memory. *Journal of Statistical Mechanics: Theory and Experiment*, 2012, P03003.

1104 Wouters, J. and V. Lucarini, 2013: Multi-level Dynamical Systems: Connecting the Ruelle
1105 Response Theory and the Mori-Zwanzig Approach, *J. Stat. Phys.* 151, 850-860.

1106 Yano, J.-I., 2014: Formulation structure of mass-flux convection parameterization. *Dyn.
1107 Atmos. Ocean*, 67, 1-28

1108 Yano, J.-I., 2015: Scale separation. *Parameterization of Atmospheric Convection*, Volume I
1109 (R. S. Plant and J. I. Yano, Eds.), World Scientific, Imperial College Press, 73-99.

1110 Yano, J.-I. and R. S. Plant, 2012a: Convective quasi-equilibrium. *Rev. Geophys.*, 50,
1111 RG4004, doi:10.1029/2011RG000378.

1112 Yano, J.-I. and R. S. Plant, 2012b: Interactions between shallow and deep convection under
1113 a finite departure from convective quasi-equilibrium. *JAS*, 69, 3463-3470.

1114 Yano, J.-I., L. Bengtsson, J.-F. Geleyn, and R. Brozkova, 2015: Towards a unified and self-
1115 consistent parameterization framework. *Parameterization of Atmospheric Convection*,
1116 Volume II (R. S. Plant and J. I. Yano, Eds.), World Scientific, Imperial College Press, 423-
1117 435.

1118 Zidikheri, M. J. and J. S. Frederiksen, 2009: Stochastic subgrid parameterizations for
1119 simulations of atmospheric baroclinic flows. *J. Atmos. Sci.*, 66, 2844–2858.

1120 Zidikheri, M you. J. and J. S. Frederiksen, 2010a: Stochastic modelling of unresolved eddy
1121 fluxes. *Geophys. Astrophys. Fluid Dyn.*, 104, 323–348.

1122 Zidikheri, M. J. and J. S. Frederiksen, 2010b: Stochastic subgrid-scale modelling for non-
1123 equilibrium geophysical flows. *Phil. T. Roy. Soc. A*, 368, 145–160.

1124 Zwanzig R, 2001 Nonequilibrium Statistical Mechanics, Oxford University Press

1125

1126

1127 LIST OF FIGURES

1128 Figure 1: System characterized by a,c) double-potential or e,g) single-potential well and
 1129 their associated probability density functions (PDFs). If the noise is sufficiently small
 1130 (a) and under appropriate initial conditions, the system will stay in the deeper potential
 1131 well and the associated probability density function of states will have a single
 1132 maximum (b). As the amplitude of the noise increases, the system can undergo a
 1133 noise-transition and reach the secondary minimum in the potential (c) leading to a
 1134 shifted mean and increased variance in the associated probability density function (d).
 1135 A linear system characterized by a single potential well and forced by additive white
 1136 noise (e) will have a unimodal PDF. However, when forced by mutliplicative (state-
 1137 dependent) white noise (g), the noise-induced changes the single-well potential of the
 1138 unforced system, so that the effective potential including the effects of the
 1139 multiplicative noise has multiple wells and the associated PDF becomes bimodal (h).
 114042
 1141 Figure 2: Top of the atmosphere net longwave radiation (outgoing longwave radiation;
 1142 OLR) in $W m^{-2}$ in DJF for the period 1981-2010. Left: *stochphysOFF*-ERA-Interim
 1143 reanalysis, middle: System 4-reanalysis, right: System 4 – *stochphysOFF*. Significant
 1144 differences at the 95% confidence level based on a two-sided *t*-test are hatched.
 1145 Adapted from Weisheimer et al. (2014).....43
 1146 Figure 3: Relative frequencies of MJO events in each of the eight MJO phases. From
 1147 Weisheimer et al. (2014).44
 1148 Figure 4: Power spectra of averagesea surface temperature in the Nino 3.4 region in a 135
 1149 year long simulations with the Community Earth System Model. Compared to
 1150 HadISST observations (blue), the simulation has three times more power for
 1151 oscillations with periods between 2 to 4 years (left). When the simulation is repeated
 1152 with the stochastic parameterization SPPT, the temperature variability in this range is
 1153 reduced, leading to a better agreement between the simulated and observed spectra
 1154 (right). Adapted from Christensen et al. (2016)©American Meteorological
 1155 Society. Used with permission.45
 1156 Figure 5: Niño 3.4 SST root mean square error (lines) and ensemble spread (dots) according
 1157 to forecast time in EC-Earth 3 seasonal re-forecast experiments initialized in May
 1158 1993-2009 with standard (SR) or high resolution (HR) atmosphere and ocean
 1159 components, with and without activating a 3-scale SPPT perturbation method in the
 1160 atmosphere.46
 1161 Figure 6: Forecast diagnostics as a function of time for the operational (black), fixed
 1162 perturbed parameter (blue) and stochastically varying perturbed parameter (red)
 1163 ensemble forecasts. Top: Forecast bias for (a) T850 and (b) U850 shown as a fraction
 1164 of the bias for the operational system: $BIAS / BIAS_{oper}$. Bottom: Root mean square
 1165 ensemble spread (dashed lines) and root mean square error (solid lines) for (c) T850
 1166 and (d) U850. Diagnostics are averaged over the region 10S-20N, 60-180E. Adapted
 1167 from Christensen et al. (2015b)©American Meteorological Society. Used with
 1168 permission.47
 1169 Figure 7: The right tail of the probability density function of summer season hourly
 1170 precipitation from a 50-member ensemble of one year single column model

1171 simulations with stochastic (blue) and conventional parameterizations (black) and
1172 fifteen years of observations (green) over a model grid box encompassing the US
1173 Department of Energy’s (DOE) Atmospheric Radiation Measurement (ARM)
1174 program’s site in Lamont, Oklahoma. The large-scale forcing for the single column
1175 model simulations are generated from a present day CESM simulation at a spatial
1176 resolution of about $2.8^{\circ} \times 2.8^{\circ}$. Adapted from Langan et al. (2014) ©Elsevier. Used
1177 with permission.....48

1178 Figure 8: Maps of the century-mean net upward water flux (mm/day) at the sea surface in
1179 (a) a control integration of a coupled climate model. (b) Difference from the control
1180 for an experiment in which the net fresh water flux across the air-sea interface is
1181 stochastically perturbed before being passed to the ocean. (c) Difference from the
1182 control for an experiment in which the net heat flux across the air-sea interface is
1183 stochastically perturbed before being passed to the ocean. From Williams
1184 (2012)©American Geophysical Union. Used with permission.....49

1185 Figure 9: Top: Amplitude of fluctuations of the eddy forcing as measured by the standard
1186 deviation of divergence of eddy flux in a 1/10 degree OGCM. Bottom: Mean eddy
1187 forcing measured by the magnitude of the mean divergence of eddy heat flux in the
1188 same heatCM. The amplitude of the fluctuations is about one order of magnitude
1189 larger than the mean eddy forcing. Adapted from Li and von Storch (2013)©American
1190 Meteorological Society. Used with permission.50

1191 Figure 10: Difference in mean standard deviation of sea ice thickness forecasts (meters)
1192 between ensembles generated by stochastic ice strength as well as atmospheric initial
1193 perturbations (STOINI) and ensembles generated solely by atmospheric initial
1194 perturbations (INI), averaged for days (left) 1 to 10, (middle) 11 to 30, and (right) 31
1195 to 90 after initialization at 00 UTC on 1 January. Stippled areas indicate differences
1196 statistically significant at the 5% level, using a two-tailed *F* test. Note the different
1197 contour intervals. Adapted from Juricke et al. (2014)©American Geophysical Union.
1198 Used with permission.....51

1199 Figure 11: Histograms of the subgrid cloud-base mass flux, resulting from the stochastic
1200 shallow cumulus cloud scheme (STOCH) and coarse-grained large-eddy simulation
1201 (LES), are compared for three horizontal grid resolutions of 1.6 km, 3.2 km and 12.8
1202 km. Adapted from Sakradzija et al. (2015).52

1203 Figure 12: Snapshot of the spatial field of convective states obtained from Large Eddy
1204 Simulation data. The distinction between the various convective states was based on
1205 cloud top height and rainwater content. Adapted from Dorrestijn et al. (2013a).....53

1206 Figure 13: Climate responses of global mean temperature to a CO₂ doubling (2x CO₂
1207 minus 1x CO₂) obtained from the ECHAM5/MPIOM-experiments with different
1208 representations of small-scale fluctuations: 'diffus' refers to experiments in which the
1209 strength of horizontal diffusion is varied; 'noise' refers to experiments in which white
1210 noise is added to small scales of the atmospheric model ECHAM5. From Seiffert and
1211 von Storch (2008)©American Geophysical Union. Used with permission.54

1212 Figure 14: (Left) The response in mean streamfunction variance of a barotropic-vorticity-
1213 equation to an anomalous vorticity forcing at latitude 45N and longitude 210E
1214 projected onto 90 EOFs (left,) the simulation of this response by a (middle) 90-EOF
1215 climate model with unmodified SGS parameterization (relative error 0.527), and by a
1216 (right) climate model with SGS parameterization corrected by FDT (relative error

| | | |
|------|---|----|
| 1217 | 0.342). Adapted from Achatz et al. (2014)©American Meteorological Society. Used | |
| 1218 | with permission..... | 55 |
| 1219 | Figure 15: Top: Comparison of the upper level kinetic energy spectra of a two level | |
| 1220 | benchmark simulation (dashed line) with associated LES (solid line) at various | |
| 1221 | resolutions for: atmospheric isotropic stochastic (isoS) LES (top spectra); atmospheric | |
| 1222 | isotropic deterministic (isoD) LES (second spectra); atmospheric deterministic scaling | |
| 1223 | law (lawD) LES (third spectra); oceanic stochastic scaling law (lawS) LES (forth | |
| 1224 | spectra); and oceanic deterministic scaling law LES (bottoms spectra).Top spectra has | |
| 1225 | the correct kinetic energy, with the others shifted down for clarity..... | 56 |
| 1226 | | |

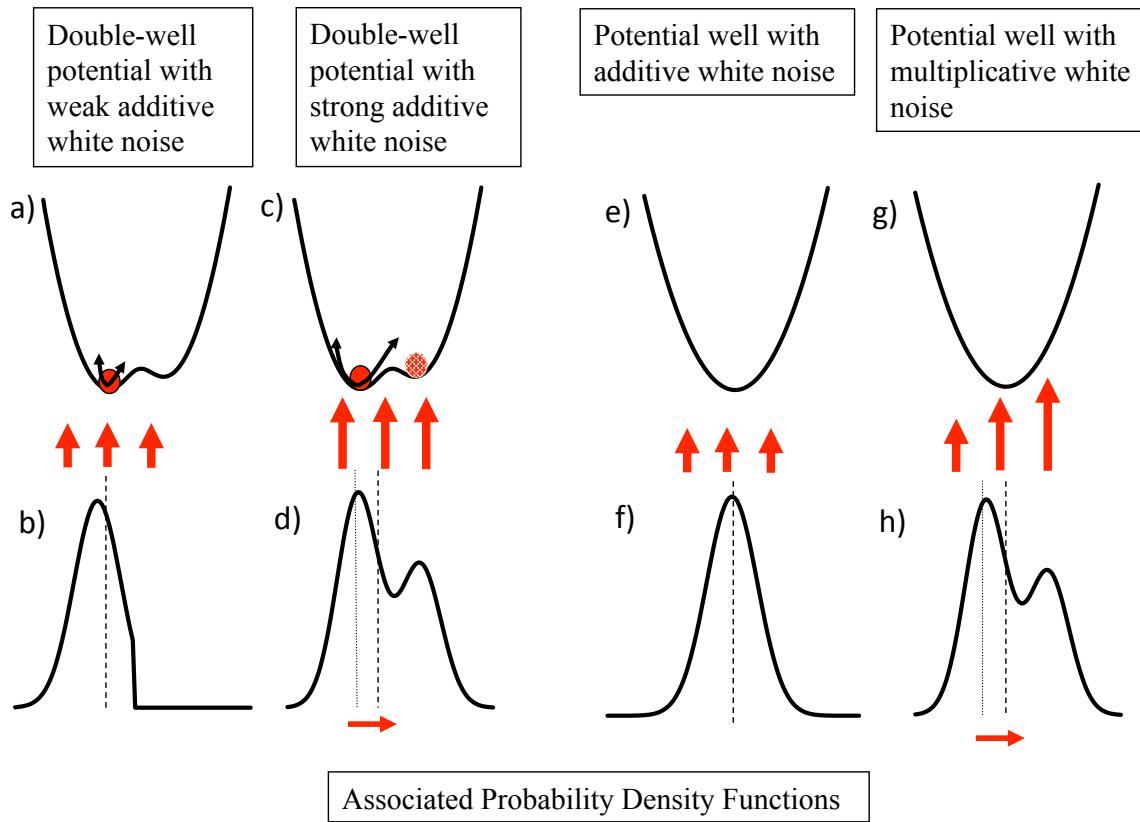


Figure 1: System characterized by a,c) double-potential or e,g) single-potential well and their associated probability density functions (PDFs). If the noise is sufficiently small (a) and under appropriate initial conditions, the system will stay in the deeper potential well and the associated probability density function of states will have a single maximum (b). As the amplitude of the noise increases, the system can undergo a noise-transition and reach the secondary minimum in the potential (c) leading to a shifted mean and increased variance in the associated probability density function (d). A linear system characterized by a single potential well and forced by additive white noise (e) will have a unimodal PDF. However, when forced by mutliplicative (state-dependent) white noise (g), the noise-induced changes the single-well potential of the unforced system, so that the effective potential including the effects of the multiplicative noise has multiple wells and the associated PDF becomes bimodal (h).

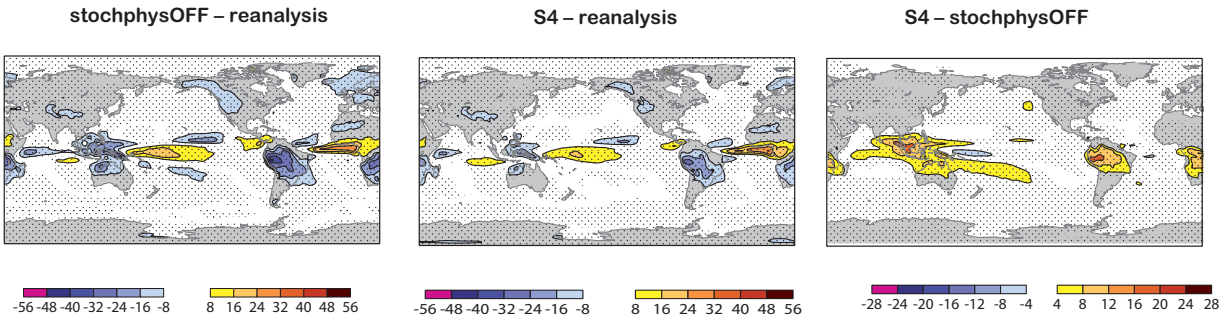


Figure 2: Bias in the top of the atmosphere net longwave radiation (outgoing longwave radiation) in $W m^{-2}$ in DJF for the period 1981-2010. Simulations are conducted with ECMWF's seasonal forecasting System 4 with (S4) and without (*stochphysOFF*) stochastic parameterizations. Left and middle panels show difference from ERA-Interim reanalysis, right panel difference between experiments. Significant differences at the 95% confidence level based on a two-sided t -test are hatched. Adapted from Weisheimer et al. (2014).

1229

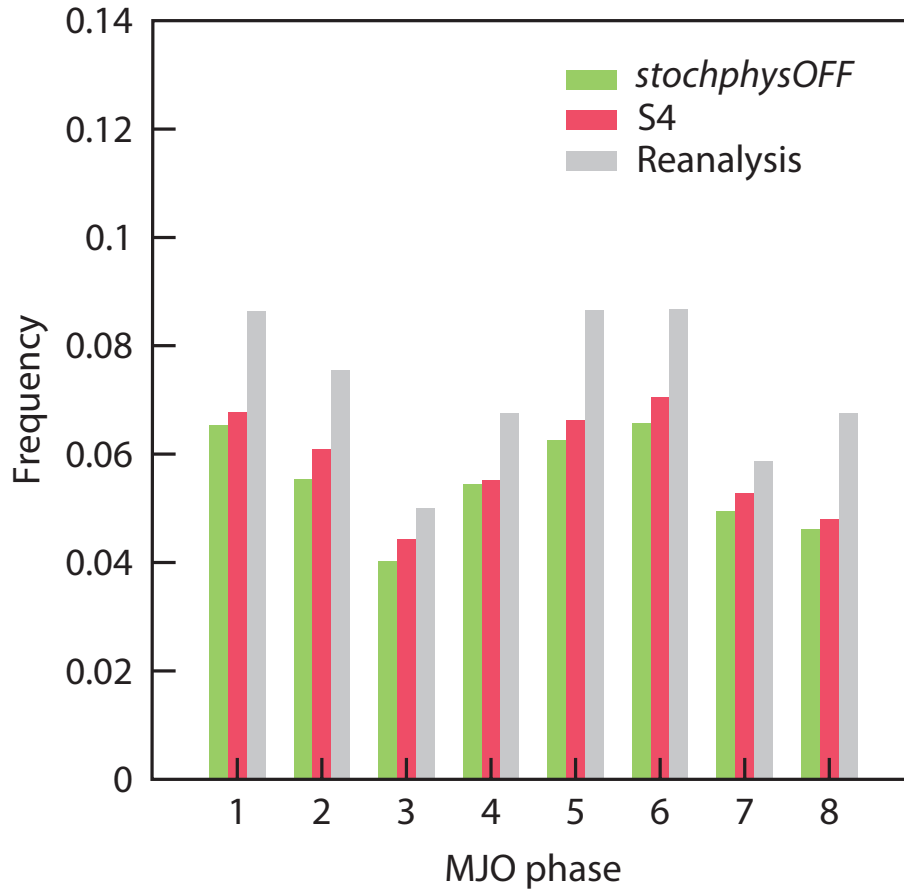


Figure 3: Relative frequencies of MJO events in each of the eight MJO phases for the period 1981-2010. Simulations are conducted with ECMWF’s seasonal forecasting System 4 with (red) and without (green) stochastic parameterizations. Relative frequencies in ERA-Interim reanalysis in are shown in grey. From Weisheimer et al. (2014).

1230

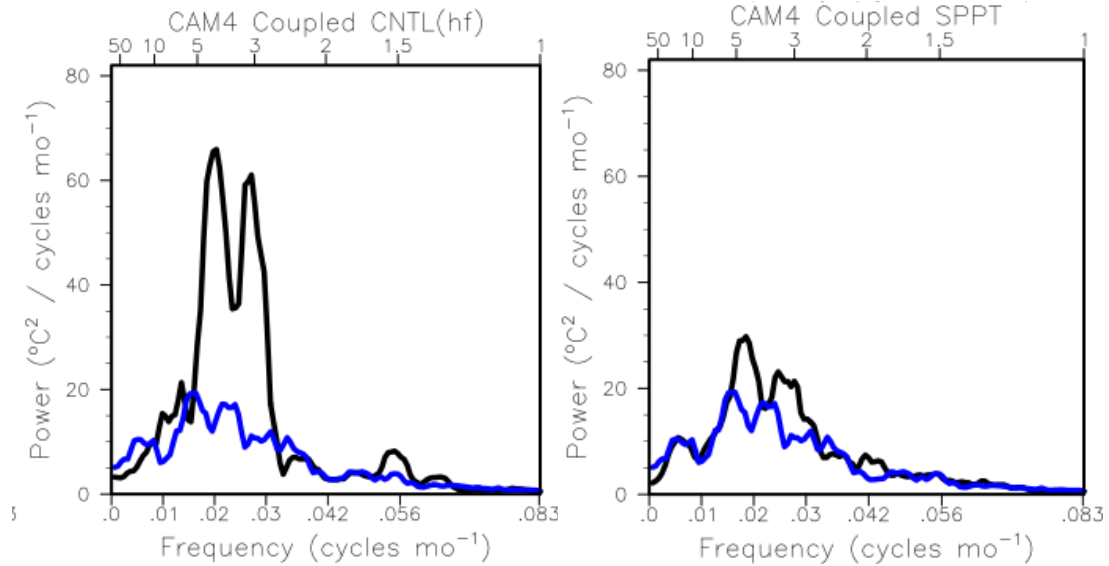


Figure 4: Power spectra of average sea surface temperature in the Nino 3.4 region in 135 year long simulations with the Community Earth System Model. Compared to HadISST observations (blue), the simulation has three times more power for oscillations with periods between 2 to 4 years (left). When the simulation is repeated with the stochastic parameterization SPPT, the temperature variability in this range is reduced, leading to a better agreement between the simulated and observed spectra (right). Adapted from Christensen et al. (2016)©American Meteorological Society. Used with permission.

1231

RMSE and spread over NINO 3.4

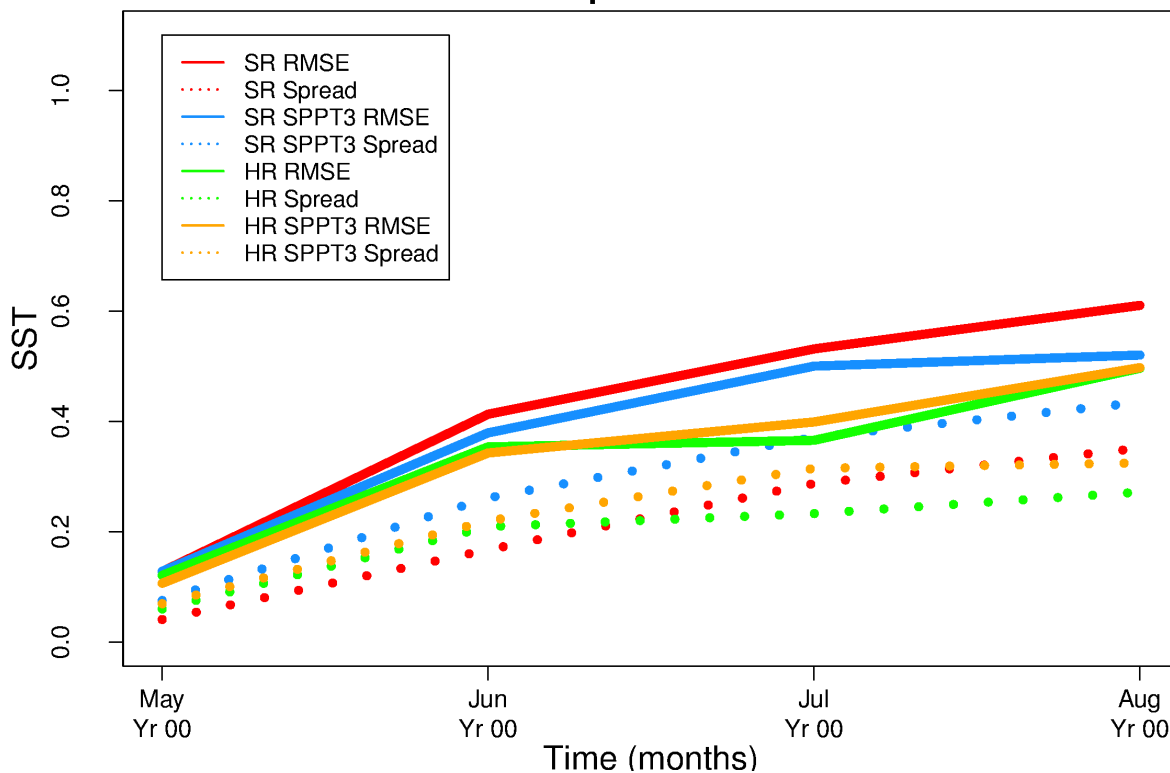
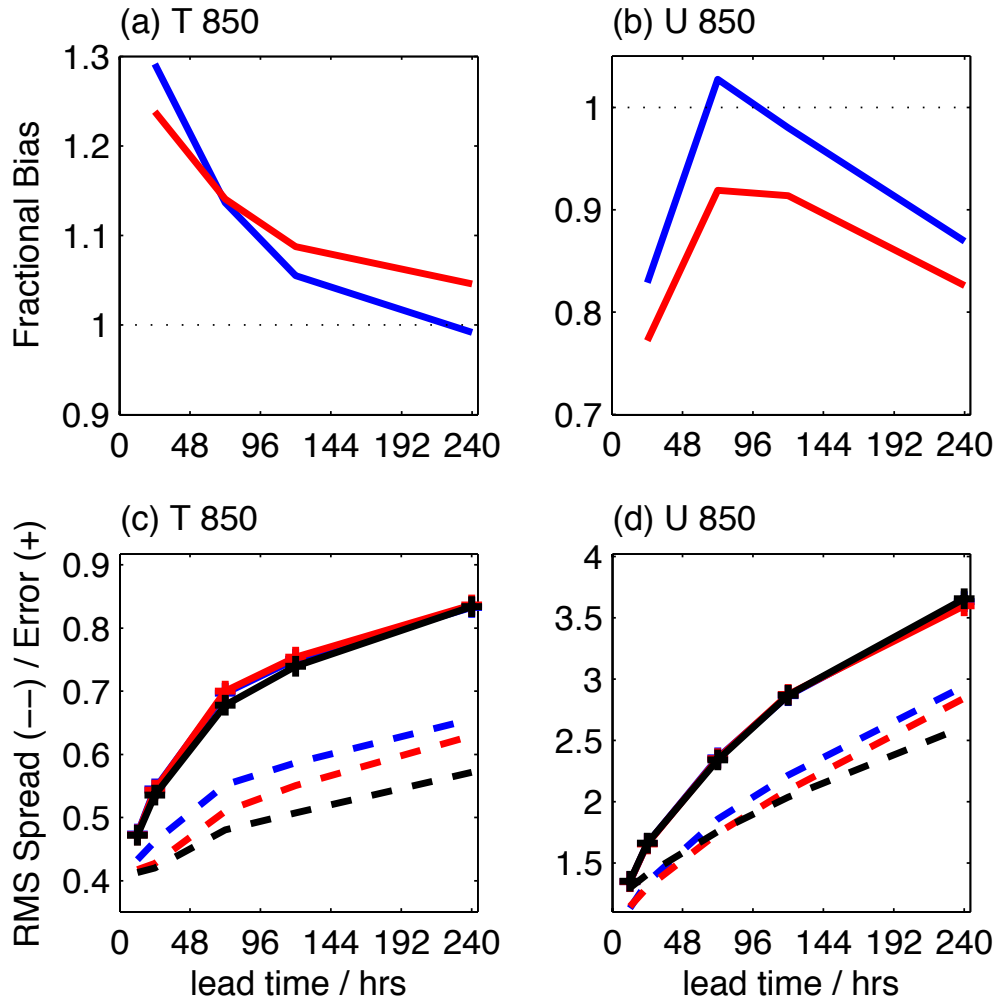


Figure 5: Niño 3.4 SST root mean square error (lines) and ensemble spread (dots) according to forecast time in EC-Earth 3 seasonal re-forecast experiments initialized in May 1993-2009 with standard (SR) or high resolution (HR) atmosphere and ocean components, with and without activating a 3-scale SPPT perturbation (SPPT3) method in the atmosphere.



1232
 1233 Figure 6: Forecast diagnostics as a function of time for the operational ECMWF IFS
 1234 (black), fixed perturbed parameter (blue) and stochastically varying perturbed parameter
 1235 (red) ensemble forecasts. Top: Forecast bias for (a) T850 and (b) U850 shown as a fraction
 1236 of the bias for the operational system: $\text{BIAS} / \text{BIAS}_{\text{oper}}$. Bottom: Root mean square
 1237 ensemble spread (dashed lines) and root mean square error (solid lines) for (c) T850 and (d)
 1238 U850. Diagnostics are averaged over the region 10S-20N, 60-180E. Adapted from
 1239 Christensen et al. (2015b)©American Meteorological Society. Used with permission.

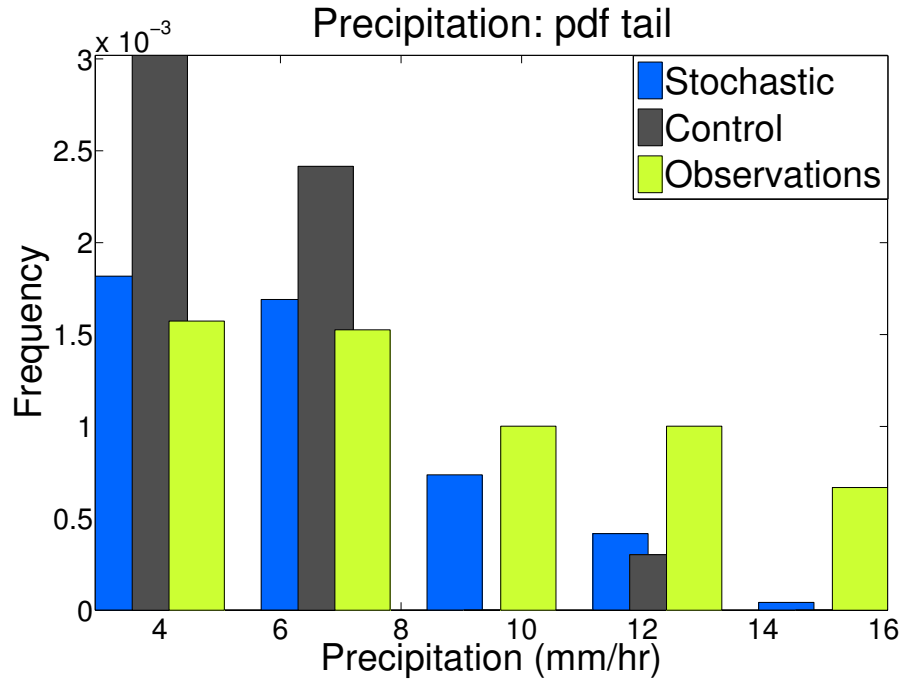


Figure 7: The right tail of the probability density function of summer season hourly precipitation from a 50-member ensemble of one year single column model simulations with stochastic (blue) and conventional parameterizations (black) of land cover over a model grid box encompassing the US Department of Energy’s Atmospheric Radiation Measurement program’s site in Lamont, Oklahoma. Observations are shown in green. The large-scale forcing for the single column model simulations are generated from a present day CESM simulation at a spatial resolution of about $2.8^{\circ} \times 2.8^{\circ}$. Adapted from Langan et al. (2014) ©Elsevier. Used with permission.

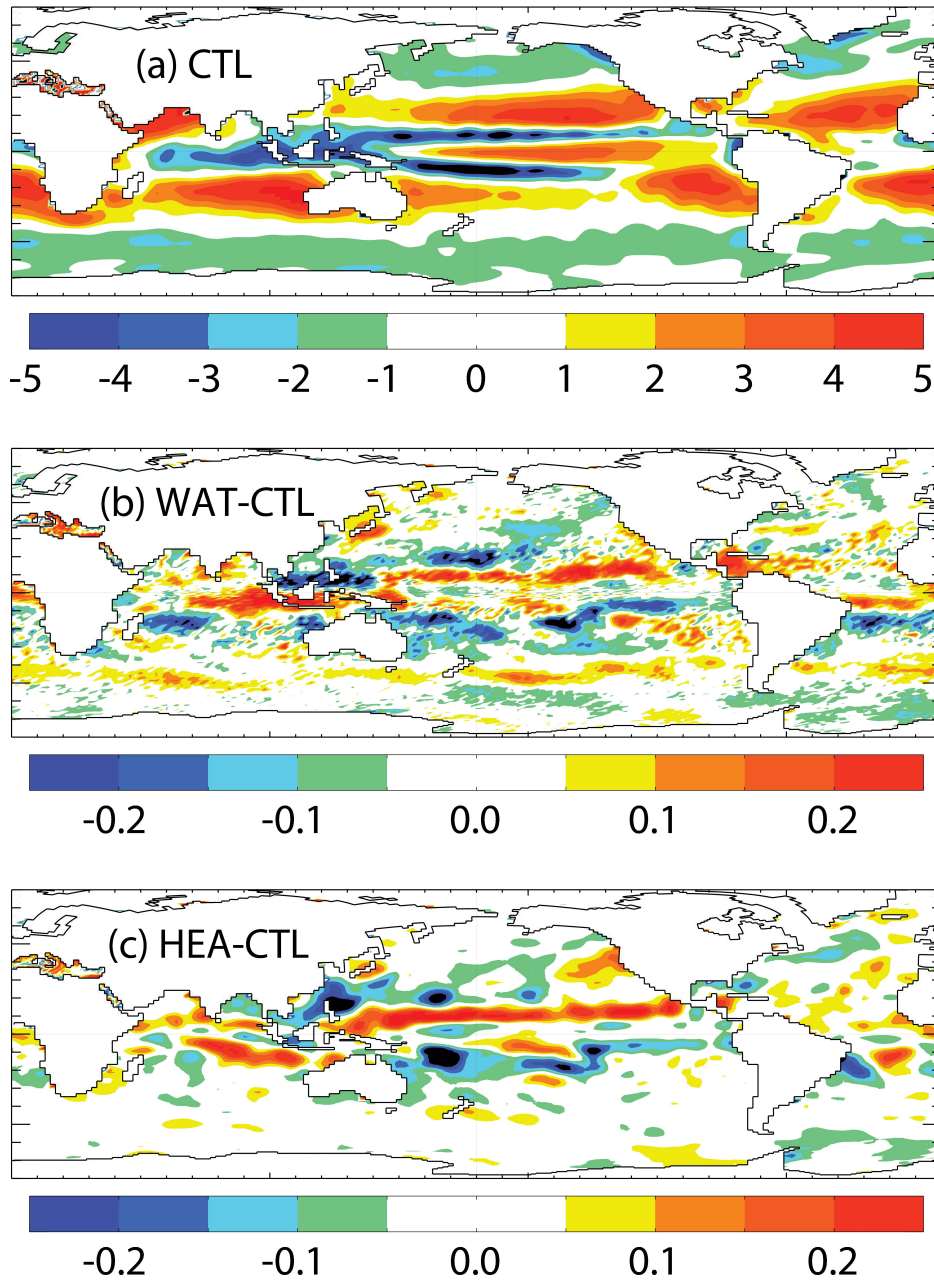


Figure 8: Maps of the century-mean net upward water flux (mm/day) at the sea surface in (a) a control integration of a coupled climate model. (b) Difference from the control for an experiment in which the net fresh water flux across the air-sea interface is stochastically perturbed before being passed to the ocean. (c) Difference from the control for an experiment in which the net heat flux across the air-sea interface is stochastically perturbed before being passed to the ocean. From Williams (2012)©American Geophysical Union. Used with permission.

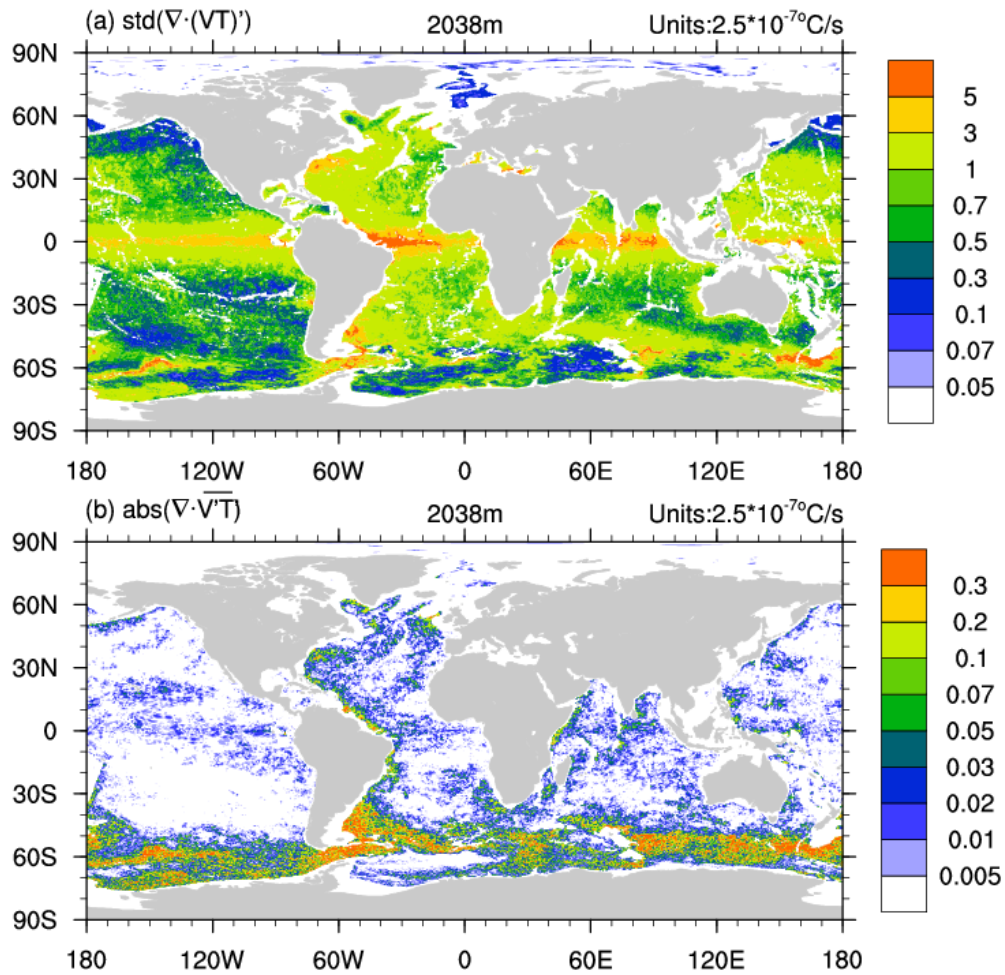


Figure 9: Top: Amplitude of fluctuations of the eddy forcing as measured by the standard deviation of divergence of eddy flux in a 1/10 degree OGCM. Bottom: Mean eddy forcing measured by the magnitude of the mean divergence of eddy heat flux in the same OGCM. The amplitude of the fluctuations is about one order of magnitude larger than the mean eddy forcing. Adapted from Li and von Storch (2013)©American Meteorological Society. Used with permission.

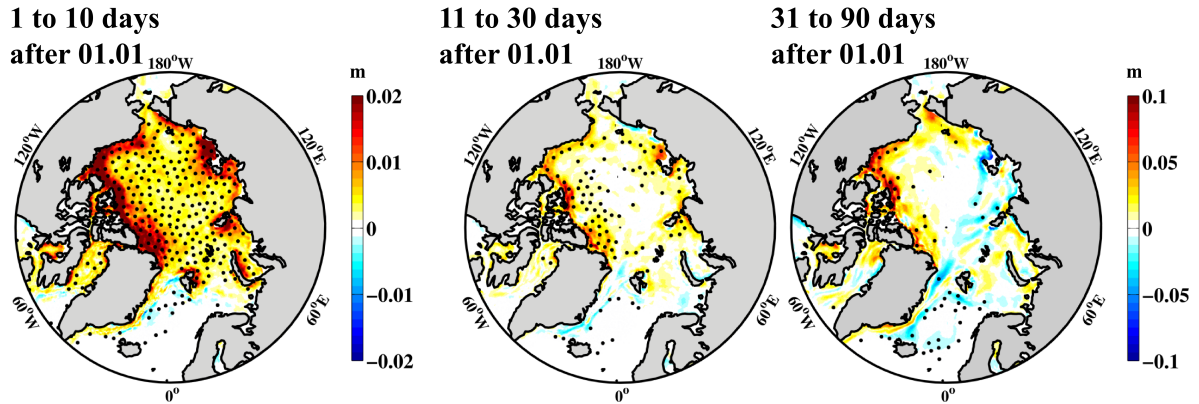


Figure 10: Difference in mean standard deviation of sea ice thickness forecasts (meters) between ensembles generated by stochastic ice strength as well as atmospheric initial perturbations and ensembles generated solely by atmospheric initial perturbations, averaged for days (left) 1 to 10, (middle) 11 to 30, and (right) 31 to 90 after initialization at 00 UTC on 1 January. Stippled areas indicate differences statistically significant at the 5% level, using a two-tailed F test. Note the different contour intervals. Adapted from Juricke et al. (2014)©American Geophysical Union. Used with permission.

1241
1242

1243

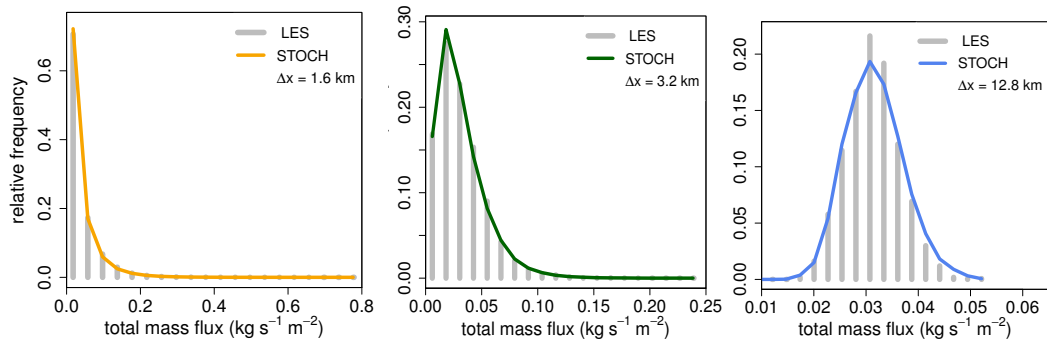


Figure 11: Histograms of the subgrid cloud-base mass flux, resulting from the stochastic shallow cumulus cloud scheme (STOCH) and coarse-grained large-eddy simulation (LES), are compared for three horizontal grid resolutions of 1.6 km, 3.2 km and 12.8 km. Adapted from Sakradzija et al. (2015).

1244

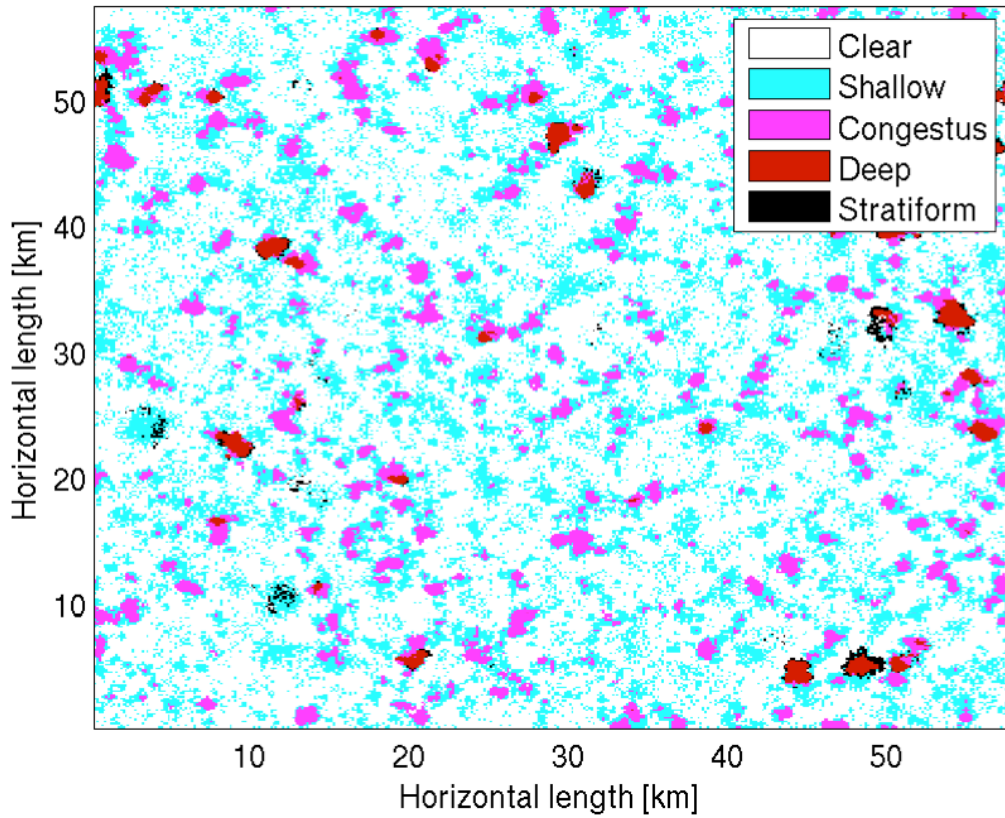


Figure 12: Snapshot of the spatial field of convective states obtained from Large Eddy Simulation data. The distinction between the various convective states was based on cloud top height and rainwater content. Adapted from Dorrestijn et al. (2013a).

1245

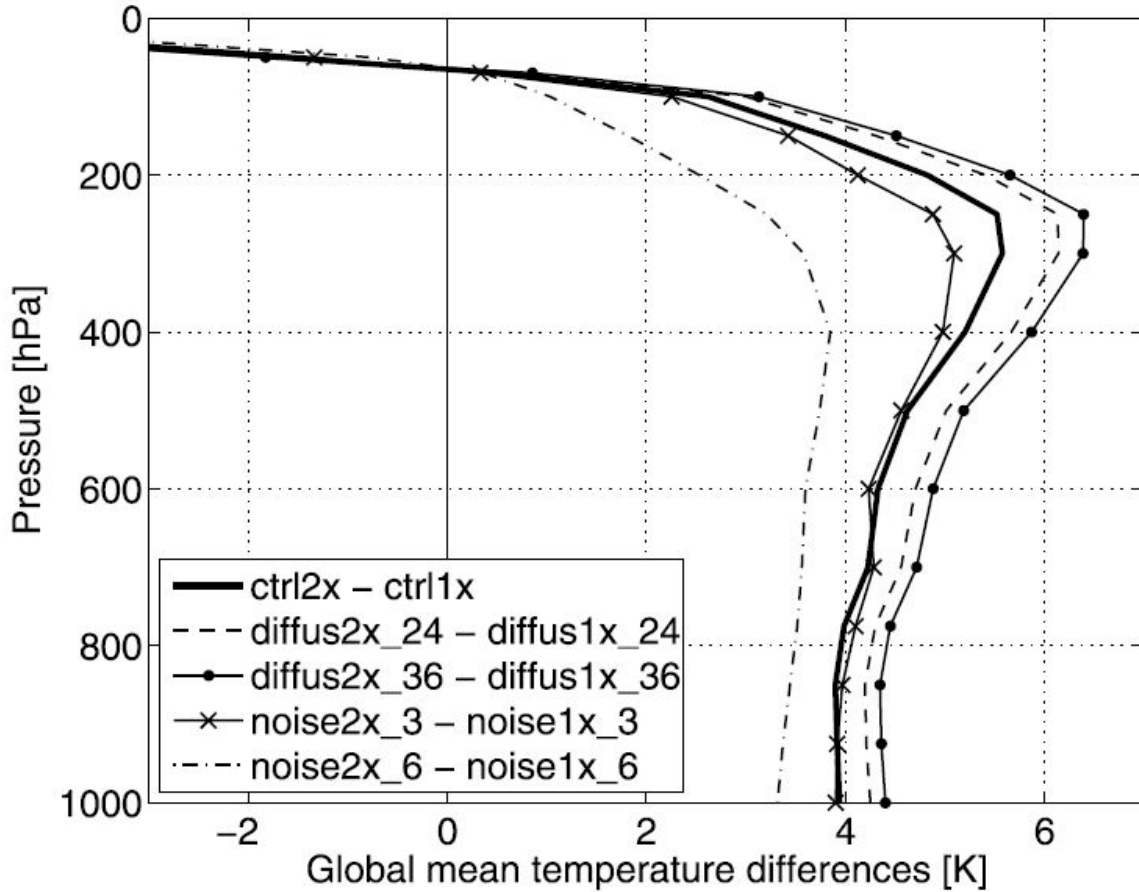


Figure 13: Climate responses of global mean temperature to a CO₂ doubling (2x CO₂ minus 1x CO₂) obtained from the ECHAM5/MPIOM-experiments with different representations of small-scale fluctuations: 'diffus' refers to experiments in which the strength of horizontal diffusion is varied; 'noise' refers to experiments in which white noise is added to small scales of the atmospheric model ECHAM5. From Seiffert and von Storch (2008)©American Geophysical Union. Used with permission.

1246

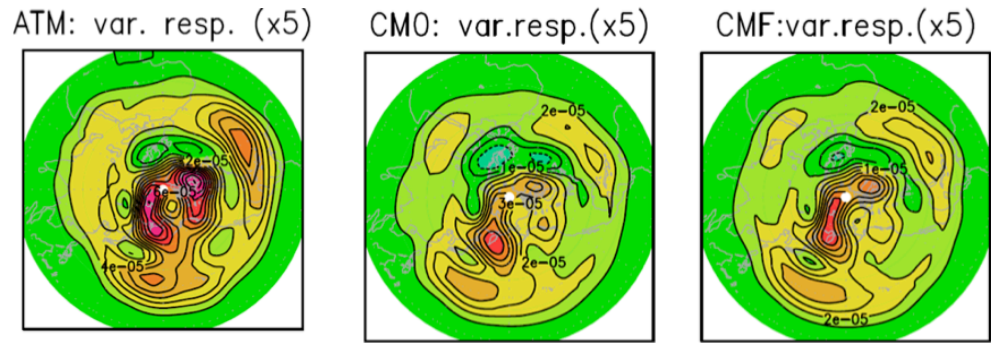


Figure 14: (Left) The response in mean streamfunction variance of a barotropic-vorticity-equation to an anomalous vorticity forcing at latitude 45N and longitude 210E projected onto 90 EOFs (left). The simulation of this response by a (middle) 90-EOF climate model with unmodified subgrid-scale parameterization (relative error 0.527), and by a (right) climate model with subgrid-scale parameterization corrected by FDT (relative error 0.342). Adapted from Achatz et al. (2014)©American Meteorological Society. Used with permission.

1247

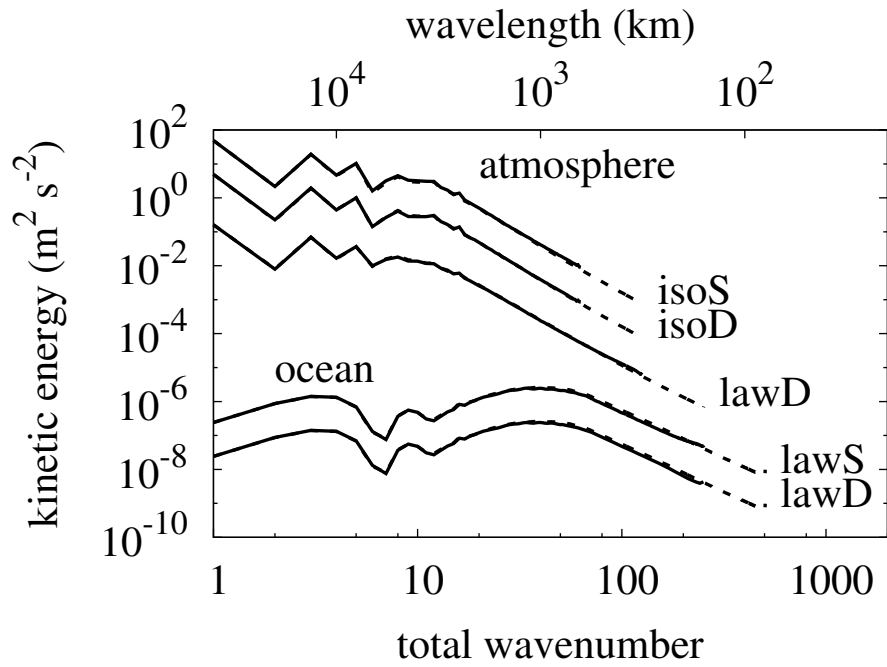


Figure 15: Top: Comparison of the upper level kinetic energy spectra of a two level benchmark simulation (dashed line) with associated LES (solid line) at various resolutions for: atmospheric isotropic stochastic (isoS) LES (top spectra); atmospheric isotropic deterministic (isoD) LES (second spectra); atmospheric deterministic scaling law (lawD) LES (third spectra); oceanic stochastic scaling law (lawS) LES (forth spectra); and oceanic deterministic scaling law LES (bottoms spectra). Top spectra has the correct kinetic energy, with the others shifted down for clarity.